Лазерно-плазменные ускорители для радиационных источников и фотоядерных реакций

В. Ю. Быченков

P.N.Lebedev Physical Institute of the Russian Academy of Science

14-е Черенковские чтения, ФИАН,
20.04.2021, 16:00

Трехмерная кильватерная волна. Баббл.

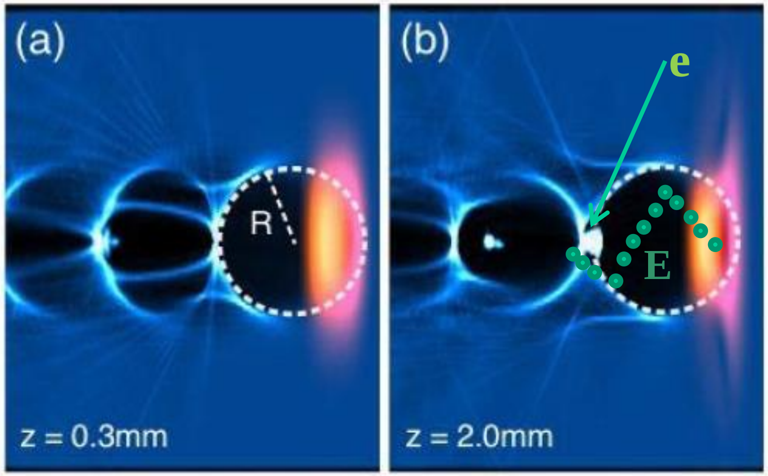

Pukhov A. and Meyer-ter-Vehn J., 2002 Appl. Phys. B 74 355

Баббл-режим

$\lambda_p(\mu\text{m}) = 2\pi c/\omega_p = 3.3\times10^{10}\,[n_e\,(\text{cm}^{-3})]^{-1/2}$

$\nabla\cdot E \sim (\omega_p/c)E \sim 4\pi e n_e,\ E \sim e n_e \lambda_p$

For $n=10^{18}$ cm^{-3}, eE=100 GeV/m

TeV collider in 10 m!

$$a_0 = \frac{v_E}{c} = \frac{eE_0}{m\omega c} \gtrsim 1$$

Корректировка на релятивизм, $a_0>1$, ➡ $E \propto n_e^{1/2} m^{1/2}$, $m \propto \gamma m_0,\ \gamma \propto a_0$, $E \propto (n_e a_0)^{1/2}$

Длина дефазировки электронов:

$$L_{dph} \approx \frac{c\lambda_p}{c-vg},\ \omega_0^2 = c^2 k_0^2 + \frac{\omega_p^2}{a_0},\ v_g = \frac{\partial\omega_0}{\partial k_0} = \frac{c}{\sqrt{1+\omega_p^2/a_0\omega_0^2}},\quad n_c \gg n,\ L_{dph} \sim \frac{n_c}{n} a_0 \lambda_p \propto \frac{a_0^{3/2}}{n^{3/2}}$$

Длина истощения импульса (etching):

$$n\,F_{pond} \times L_{dpl} \approx \frac{E_0^2}{8\pi} \equiv nmc^2 \frac{a_0^2}{2}\frac{\omega_0^2}{\omega_p^2},\ F_{pond} \sim mc^2 \nabla a_0 \sim a_0 \frac{mc^2}{c\tau},\ L_{dpl} \sim \frac{n_c}{n} c\tau a_0$$

$$E \propto \sqrt{n_e a_0} \qquad \Delta W_{dph} \sim \frac{n_c}{n} a_0^{3/2} mc^2 \qquad \Delta W_{dpl} \sim \frac{n_c^{1/2}}{4n^{1/2}} a_0^{3/2} mc^2 (\omega_0 \tau)$$

Wakefield acceleration of electrons

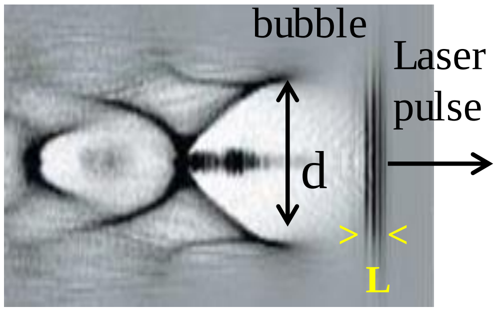

$0.004n_c$

Tajima T. and Dawson J. M. 1979 Phys. Rev. Lett. 43 267

3D plasma wave

Pukhov A. and Meyer-ter-Vehn J., 2002 Appl. Phys. B: Lasers Opt. 74 355

"bubble" regime

$L < \lambda_p$ $L < d$ R=d/2~15-20 μm I ~ $(10^{18}$-$10^{19})$W/cm^2

Quasi-monoenergetic electrons, pC charge,
up to GeV energy range in a gas jet or capillary (n_e~10^{17}-10^{19}cm^{-3})

Плотная плазма. Ультра-релятивистская интенсивность, $a_0 >> 1$

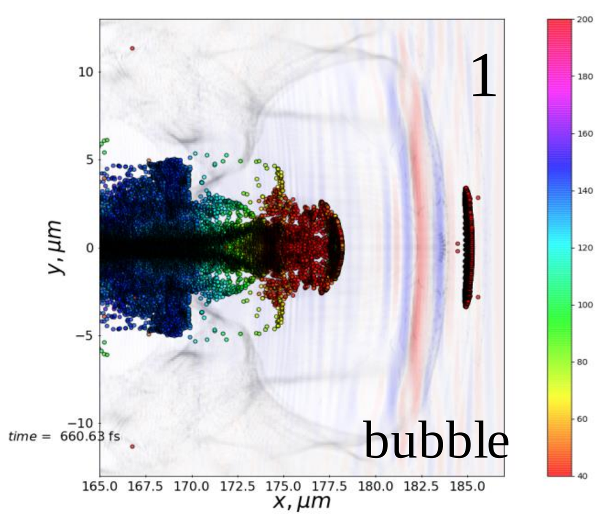

a_0 = 10, R = 10λ, τ = 13fs, n_e=0.04n_c

~~$L < \lambda_p$ $L < d$~~

L > λ_p , L > d

$E_{1L}/E_{2L} \approx 2$

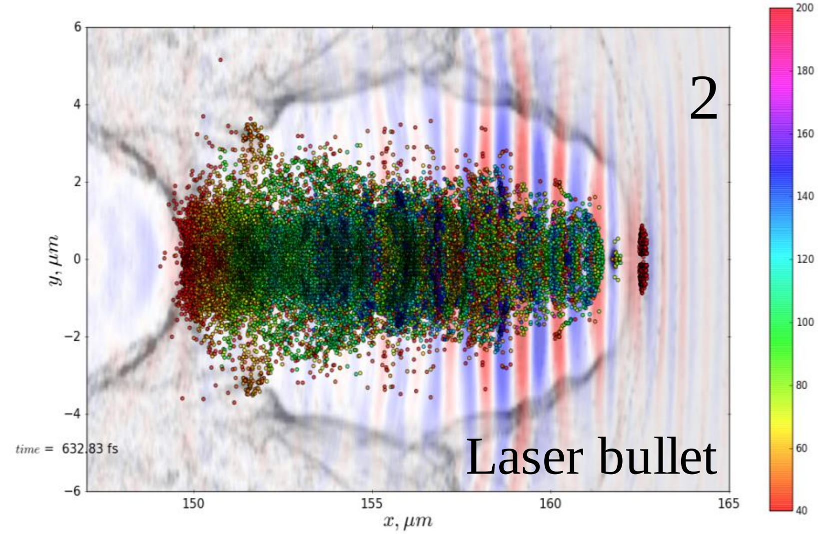

a_0 = 24, R = 2λ, τ = 30fs, n_e=0.1n_c

Световая пуля

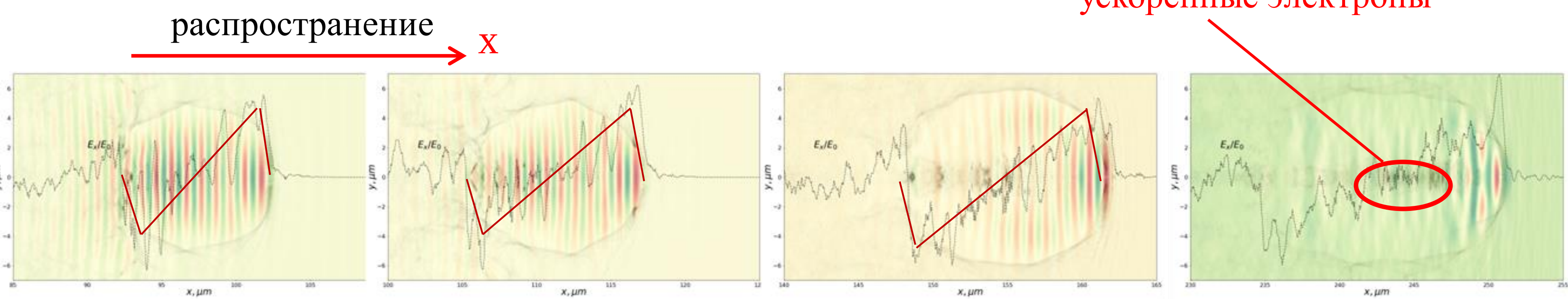

длина распространения лазерной пули >> $X_R = \omega R_L^2/c$ – рэлеевская длина

$$\text{длина истощения} \sim c\tau \frac{\omega^2}{\omega_p^2} a_0 \propto \sqrt{I}\,\tau/n_e$$

Для чего сие ?

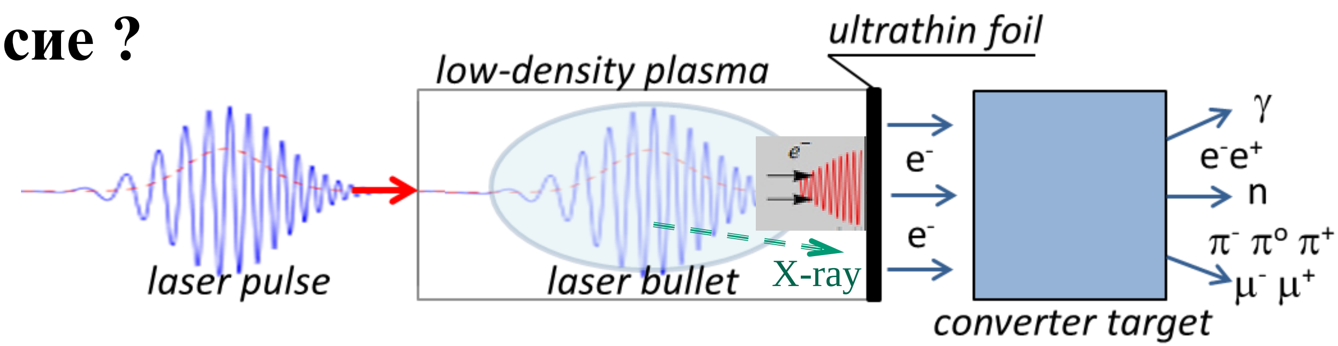

Цель: получение максимального заряда сгустка электронов ультра-релятивистской энергии

Laser light self-trapping regime

$n_e = 0.1 n_c$

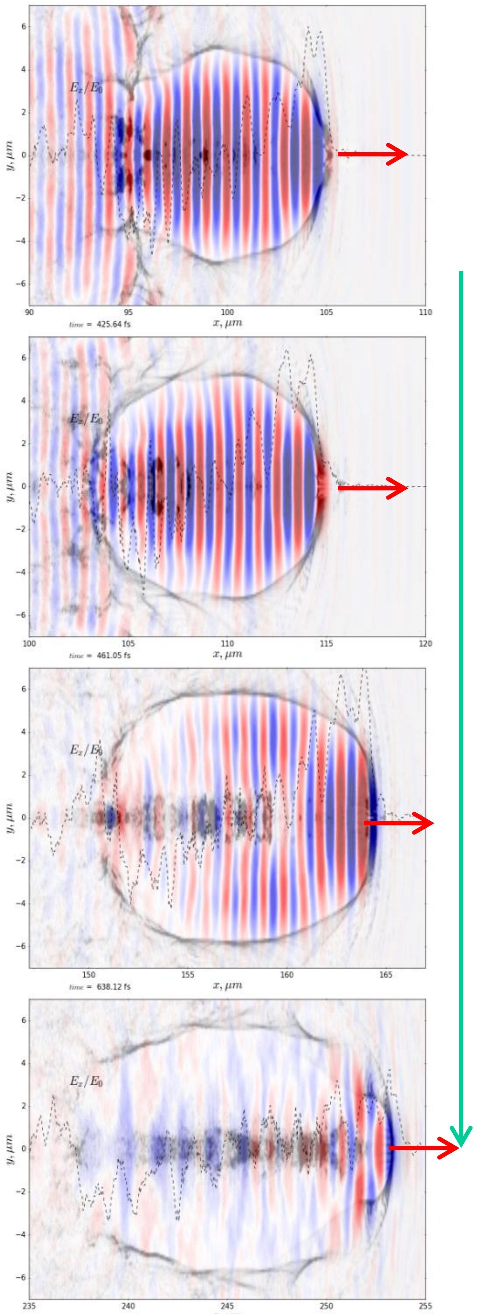

Propagation over ~ 10 Rayleigh lengths

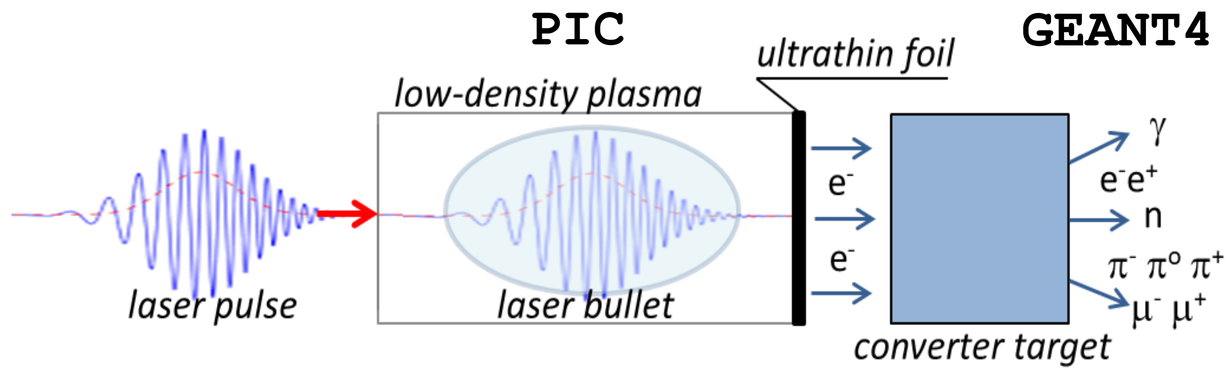

$$R \cong \frac{c}{\omega_p} \alpha \sqrt{a_0}$$

$a_0 = 0.85\lambda[\mu m]\sqrt{I[W/cm^2]} \times 10^{-9}$ α - numeric factor ~ (1-2)

$a_0 = 24$, $R_L = 2\lambda$, $\tau = 30fs$, $P = 100$ TW

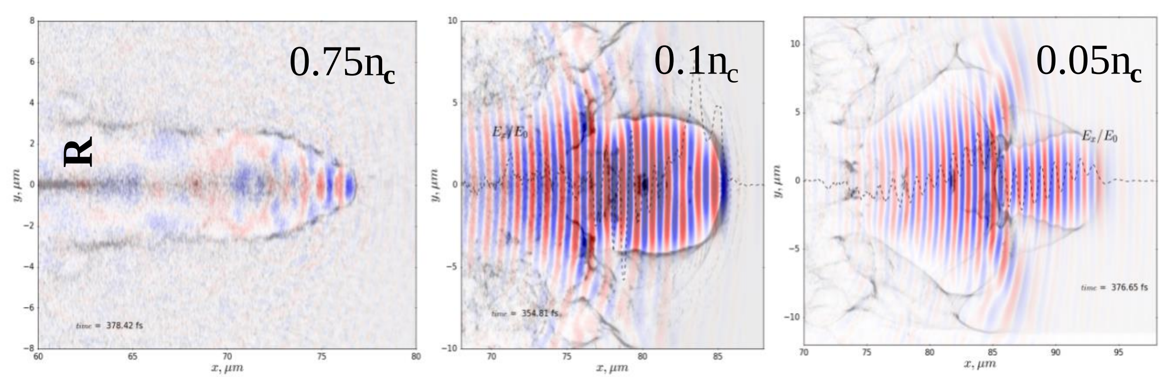

R (n, I) - matching

Matching condition ≡ relativistic (a>>1) self-trapping

Comparison of two self-trapping pulses with initial radius $R_L = 2\,\mu$m and amplitudes $a_0 = 24$ (left) and $a_0 = 72$ (right) propagating in plasmas with the corresponding electron densities $0.1n_c$ and $0.3n_c$

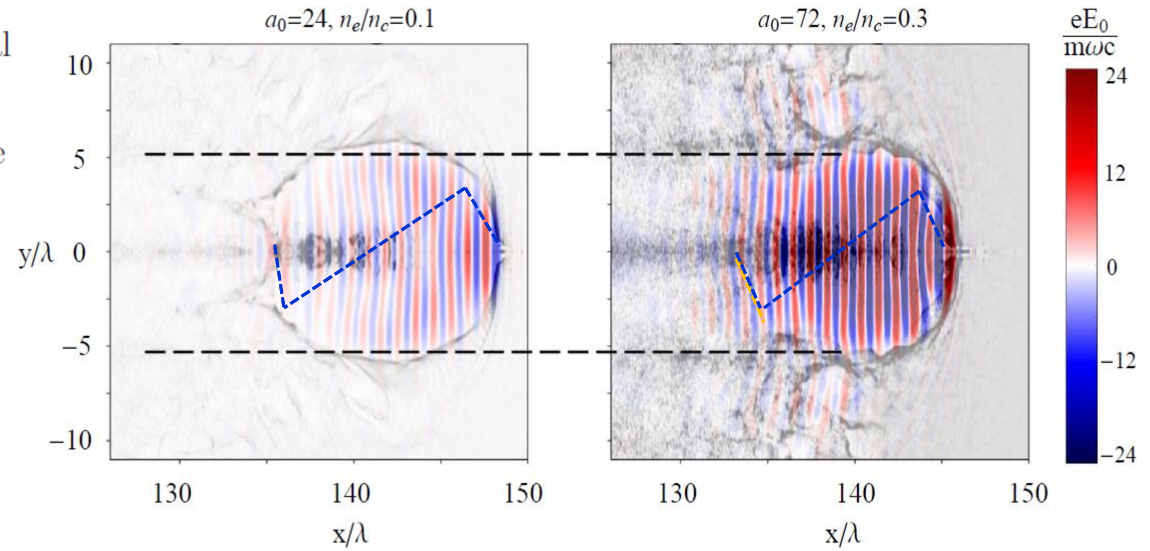

Laser pulse = soliton

$$R \sim \frac{c}{\omega_p}\sqrt{a_0}$$

$$\frac{R_1}{R_2} = \sqrt{\frac{a_1}{a_2}\frac{n_2}{n_1}}$$

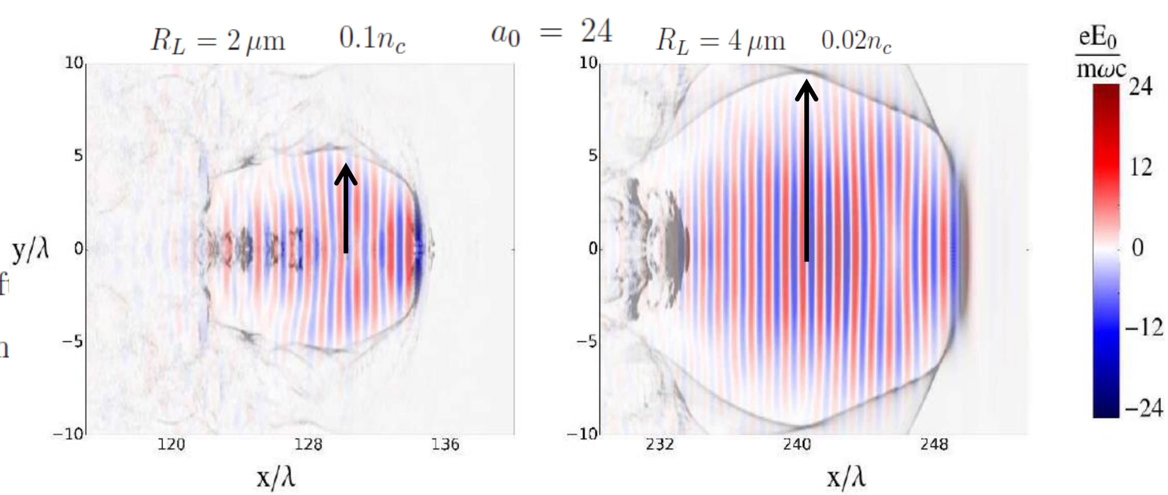

Comparison of two self-trapping pulses with the amplitude $a_0 = 24$ and initial radii $R_L = 2\,\mu$m (lef and $R_L = 4\,\mu$m (right) propagating in plasmas with the corresponding electron densities $0.1n_c$ and $0.02n_c$

M.G.Lobok, A.V.Brantov, V.F.Kovalev, and V.Yu.Bychenkov
Plasma Phys. Contr. Fus. 61, 124004 (2019)

Physics of the matched cavern spot size condition

$$R \cong \frac{c}{\omega_p}\alpha\sqrt{a_0}$$ $$R = \frac{c}{\omega}\sqrt{\frac{n_c}{n_e}}\left(\frac{16\alpha^4 P}{P_c}\right)^{1/6}$$ P – laser pulse power

1 Gordienko S and Pukhov A 2005 *Phys. Plasmas 12*, 043109 $\alpha \approx 1.12$

2 Lu M *et al* 2007 *Phys. Rev. STAB* **10**, 061301 $\alpha \approx 2$

3 Lobok M G Brantov A V Gozhev D A and Bychenkov V Yu 2018 *Plasma Phys. Control. Fusion* **60** 084010 $\alpha \approx 2$

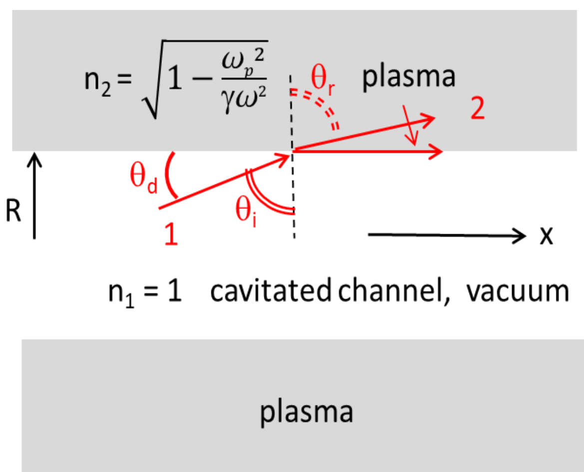

Snell's law

$$\theta_d \simeq \lambda/\pi R \qquad \theta_i = \pi/2 - \theta_d$$

$$n_1 \sin\theta_i = n_2 \sin\theta_r$$

condition of the total internal reflection, $\theta_r = \pi/2$

$$\theta_d^2 \simeq \left(\frac{2c}{\omega R}\right)^2 \simeq \frac{\omega_p^2}{\gamma\omega^2} \simeq \frac{\sqrt{2}\omega_p^2}{a_0\omega^2} \qquad \gamma = \sqrt{1 + a_0^2/2} \simeq a_0/\sqrt{2}$$

$$R \cong \frac{c}{\omega_p} 2^{3/4}\sqrt{a_0}$$

Laser beam self-trapping: plane geometry

NLSE + relativistic nonlinearity of electron mass

$$2ik\partial_z E + \partial_{xx} E + k^2 \frac{\epsilon_{\rm nl}}{\epsilon_0} E = 0,\ E = A\exp\left(i\frac{\nu z}{2kd^2}\right),\ \gamma = \sqrt{1+|E/E_{\rm rel}|^2},\quad E=E(x,z,t-z\sqrt{\varepsilon_0}/c),$$

$$\epsilon_0 = 1 - \frac{4\pi e^2 n_{e0}}{(m_0\omega^2)},\ \epsilon_{\rm nl} = \epsilon_0 \frac{k_p^2}{k^2}\left(1-\frac{1}{\gamma}\right),\ k_p^2 = \frac{4\pi e^2 n_{e0}}{m_0 c^2},\ k = \frac{\omega}{c}\sqrt{\epsilon_0},\ E_{\rm rel}^2 = \left(\frac{\omega c m_0}{e}\right)^2.$$

In dimensionless variables $z/2kd^2$, x/d, A/A_0, the solution depends upon two parameters:

$\rho = \omega_{\rm pe} d/c$ and $i_0 = (e/\omega m_0 c)^2 A_0^2 = I_0/I_r$, with $I_0 = (c/4\pi)A_0^2$, $I_r = \omega^2 m_0^2 c^3/(4\pi e^2)$.

Self-trapping solution for $\nu = \rho^2(1+(2/i_0)(1-p_0))$

$$\sqrt{\frac{2}{(p_0+1)}}\rho x = -\pi + 2\arctan\sqrt{\frac{p+1}{p_0-p}} - \sqrt{\frac{2}{p_0-1}}\ln\frac{2\sqrt{p_0-p}+\sqrt{2(p_0-1)(p+1)}}{\sqrt{2(p_0+1)(p-1)}},$$

$$p_0 = \sqrt{1+i_0},\quad p = \sqrt{1+i_0 A^2},$$

Limiting case $\quad i_0 \to 0: \quad A^2 = \cosh^{-2}\left(x\rho\sqrt{i_0}/2\right)$.

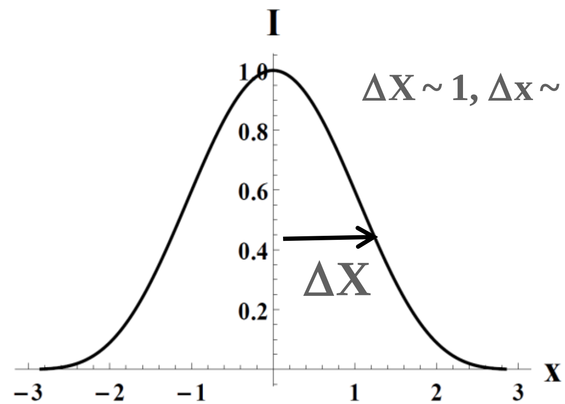

$\Delta X \sim 1,\ \Delta x \sim c a_0^{1/2}/\omega_{pe}$

$$x \equiv \sqrt{2/(p_0+1)}\rho x,\quad I \equiv A^2.$$

$$\varepsilon_2|E|^2 = \frac{\omega_p^2}{4\omega^2}\left(\frac{eE}{m_e\omega c}\right)^2$$ Таланов (1964) $$E(x) \propto \frac{1}{\cosh(x/\Delta)}$$ $$\Delta \propto \frac{m}{eE_0\omega_p} \propto \frac{1}{a_0} \to \propto \frac{m^{3/2}}{a_0} \propto a_0^{1/2}$$

Analytical theory of relativistic self-focusing

$$2ik\partial_z E + \triangle_\perp E + k^2(\epsilon_{nl}/\epsilon_0)E = 0\,,\quad E(0,\mathbf{r}) = E_0(\mathbf{r})$$

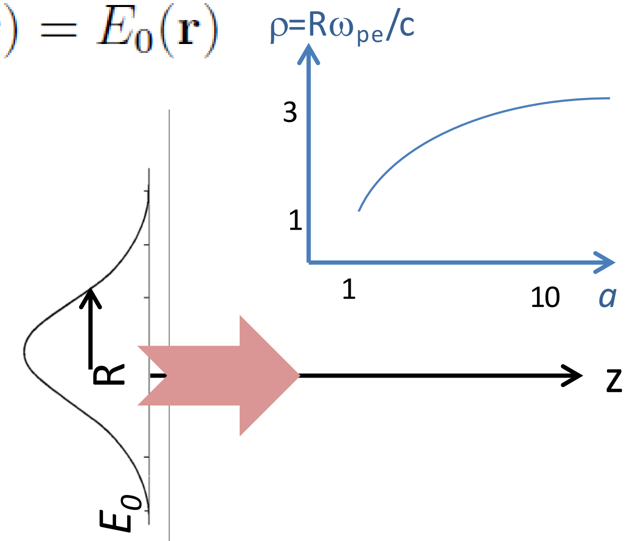

$$\epsilon_{nl} = \epsilon_0 \frac{k_p^2}{k^2}\left(1 - \frac{n_e}{\gamma n_{e0}}\right) \qquad \gamma = \sqrt{1 + |E/E_{rel}|^2}$$

$$E_{rel}^2 = (\omega c m_0/e)^2$$

$$N_e = \frac{\left(1 + k_p^{-2}\triangle_\perp \gamma\right)}{\left(1 - \exp\left(-\alpha_0\left(1 + k_p^{-2}\triangle_\perp\gamma\right)\right)\right)} \qquad n_e = n_{e0} N_e(\gamma)$$

relativistic electron mass + and ponderomotive charge-displacement

V.F.Kovalev & V.Yu.Bychenkov
Phys. Rev. E **99**, 043201 (2019)

Gaussian radial intensity distribution at the plasma boundary

- **Search for new regimes of relativistic self-focusing**

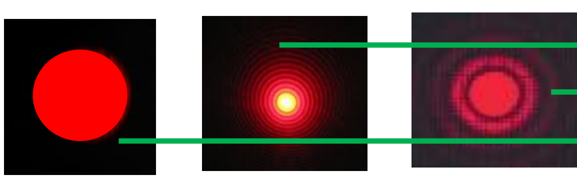

self-focusing on the axis

tubular self-focusing

self-trapping

three stationary self-focused waveguide propagation modes

- **Finding of window parameters for different regimes of channeling**

Self-trapping: $R\omega_p/c = F(a_0)$, $a_0 >> 1 \rightarrow R\omega_p/c \sim \sqrt{a_0}$ → balance of forces; → no filamentation

Intensity dependence

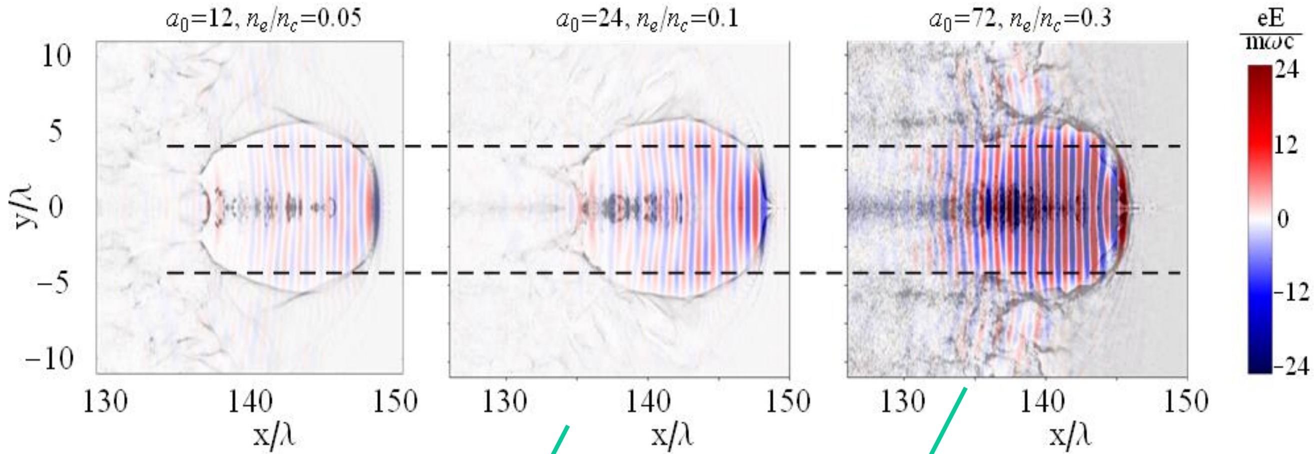

Very universal plateau-type spectra

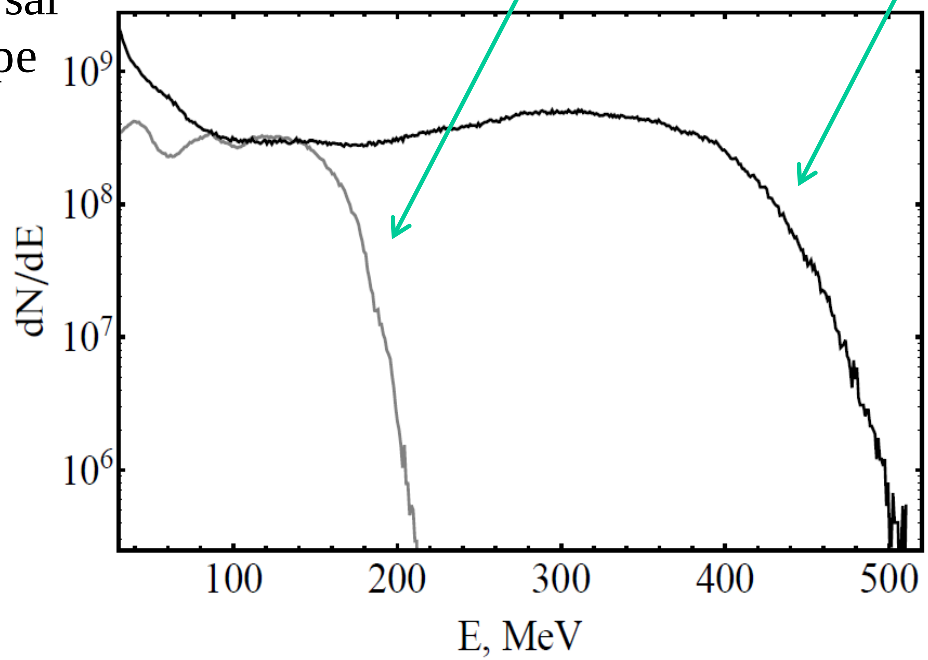

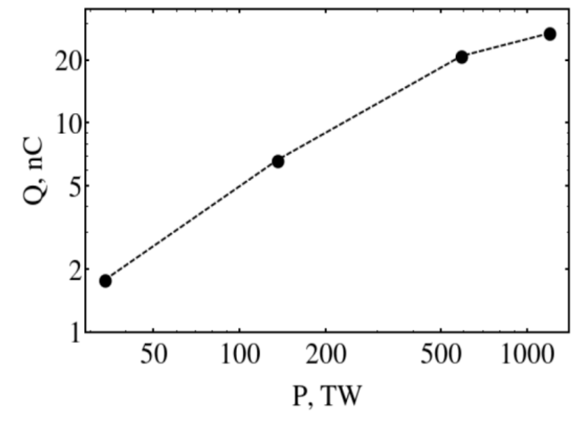

Dependence of the maximum total electron charge on the laser power for a 30 fs pulse

Какую выбрать толщину мишени?

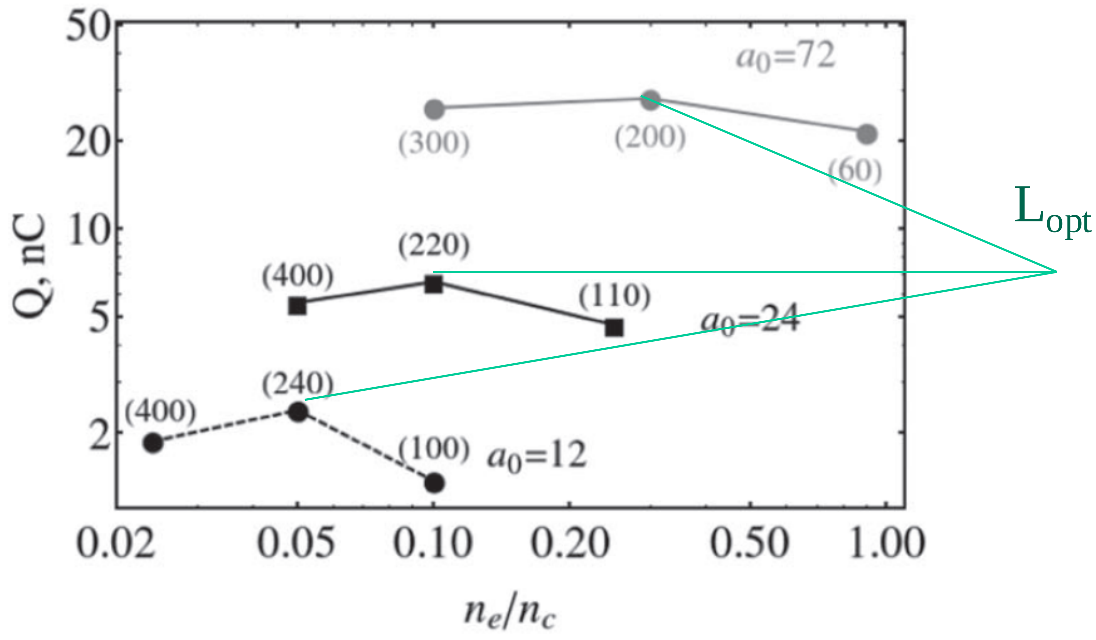

Maximum total electron charge versus target densities for 30 fs laser pulses with the amplitudes $a_0 = 72$ (gray dots), $a_0 = 24$ (black squares) and $a_0 = 12$ (black dots). The number in parentheses corresponds to the optimal target thickness in μm.

$$L_{opt} \lesssim L_{dpl} = \frac{1}{4} c\tau \frac{n_c}{n} < a_0 >$$

a_0=24, $< a_0 >$ =12, n=0.1nc, cτ=9 мкм, L_{dpl}=270 мкм

Electron spot

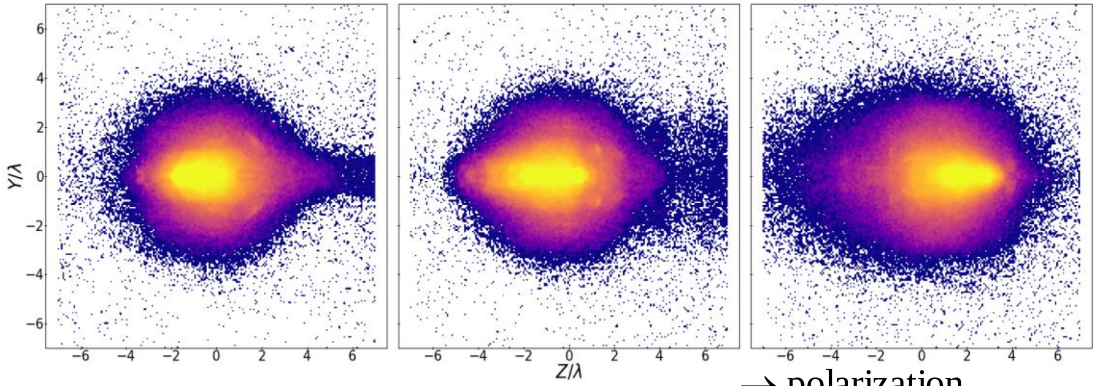

→ polarization

$\Delta z \approx 0.16\lambda a_0$

$T \approx 0.25\lambda a_0^2/c$

electron divergence is approximately 50 mrad, that corresponds to the emmitance of about 0.1 rad×μm

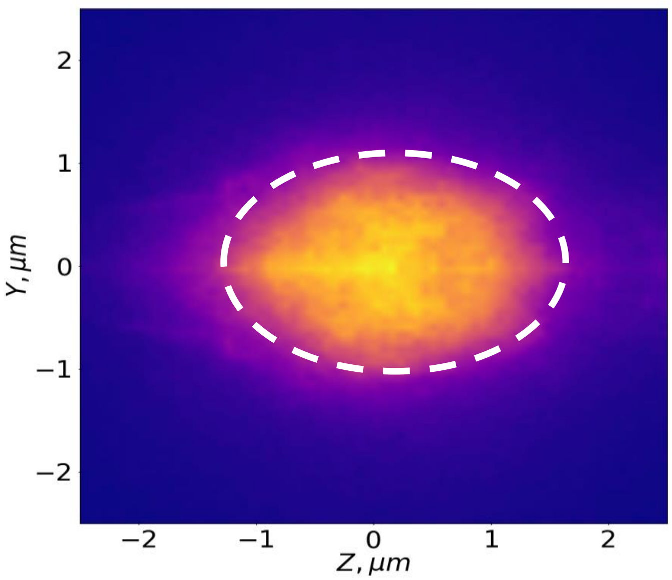

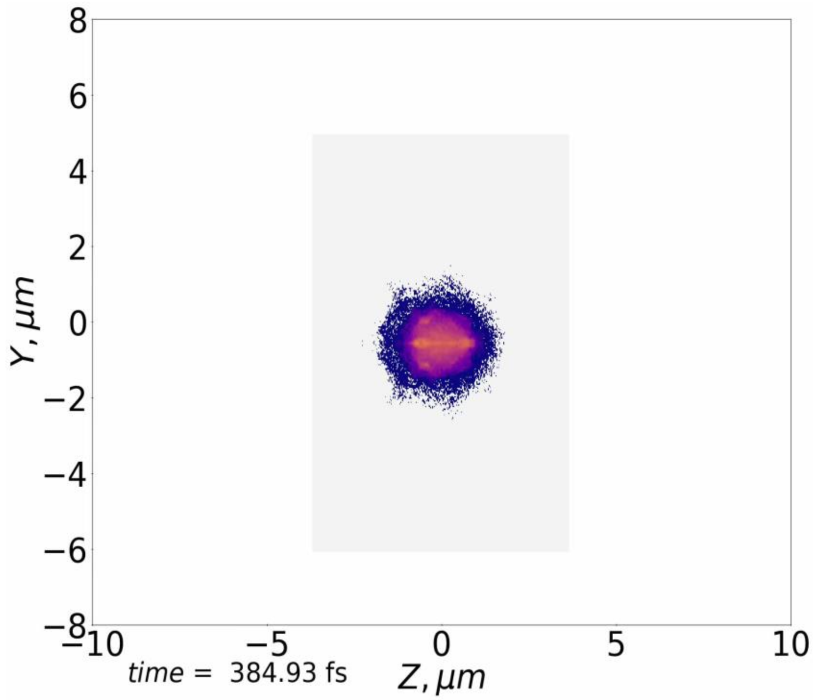

face pics

МАГАТЭ

Международное агентство по атомной энергии

IAEA
International Atomic Energy Agency
Atoms for Peace and Development

Technical Meeting on Advances in Laser Driven Neutron and X-ray Sources and their Applications

Virtual Event

8–11 February 2021

Ref. No.: EVT1905325

- Laser-based neutron and X-ray production schemes
- Measurements of matter properties with short pulsed neutron and X-rays sources
- Neutron scattering and isotope selective imaging
- Development of compact and deployable systems
- Applications with societal impact
- Analytical capacity in challenging environments and proliferation to developing countries.
- Innovative solutions for nuclear safeguards and non-proliferation
- Industry-related applications, including a) Non-destructive testing and evaluation, b) Inspection techniques, and c) Techniques to identify small quantities of materials/contaminants
- Priority research needs and instrumentation R&D
- Training in Laser Driven Neutron and X-ray Sources and their Applications.

An **International Programme Advisory Committee (IPAC)** is established for the Technical Meeting composed by the following members:

Name	Affiliation
Mr. Markus Roth	Institut für Kernphysik, Technische Universität Darmstadt, Darmstadt, Germany
Ms. Ceri Brenner	STFC Rutherford Appleton Laboratory, Didcot, Oxford, UK
Mr. Ishay Pomerantz	School of Physics and Astronomy, Tel-Aviv University, Tel Aviv, Israel
Mr. Akifumi Yogo	Institute of Laser Engineering, Osaka University, Osaka, Japan
Mr. Sven Vogel	Los Alamos Neutron Science Center, LANL, Los Alamos, NM 87545, USA

Радиационные и ядерные применения лазерно-ускоренных электронов:

Электронная радиотерапия (радиография)

Источник жесткого рентгеновского излучения

Экранированная гамма-радиография

Полностью оптический комптоновский источник

Фотоядерные реакции. Получение нейтронов

Лазерный источник элементарных частиц

Получение медицинских изотопов

Трансмутация долгоживущих изотопов

Electron beams in radiation therapy

Very High Energy Electrons - VHEE

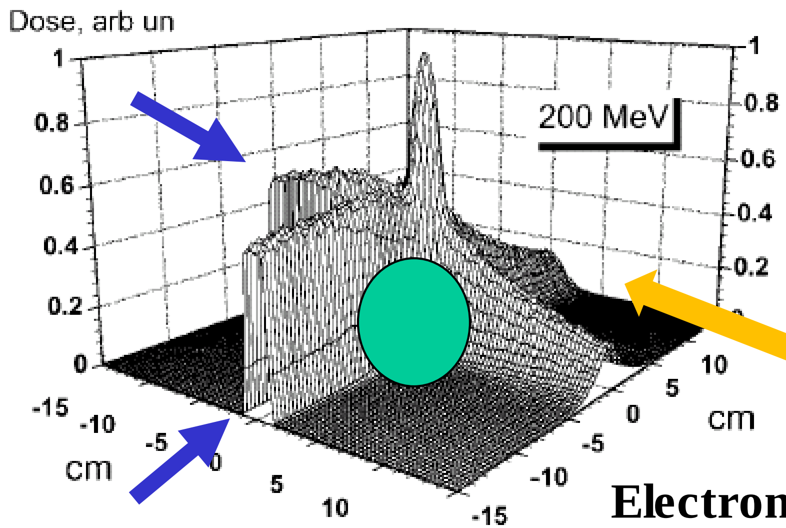

Electron beam

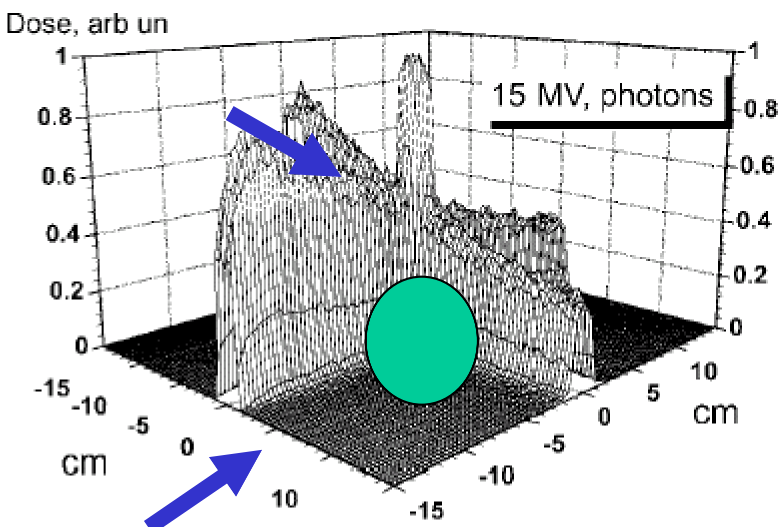

15 MV clinical accelerator x-ray beam

Current status

current clinical level linear accelerators ~ 6–30 MeV

intra-operatory radiation therapy

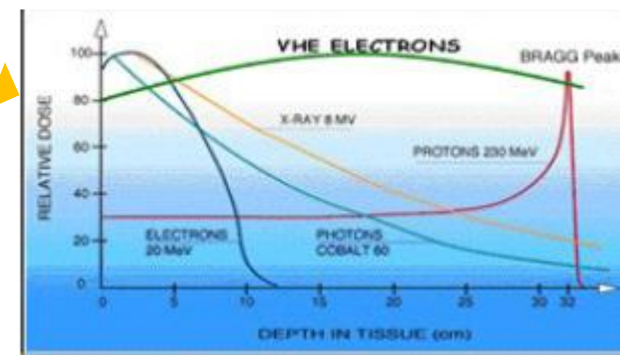

Dose deposition

C. DesRosierset al., Phys. Med. Biol. **45,** 1781 (2000)

Experiment on “radiotherapy” with VHEE electrons

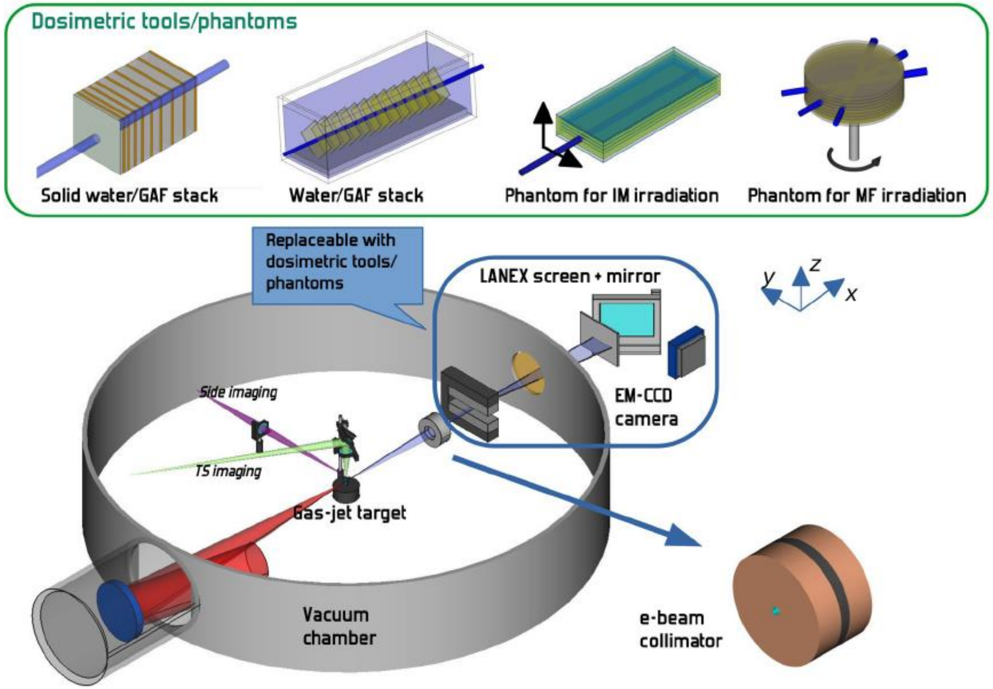

L. Labate et al., Scientific Reports **10**:17307, (2020)
220 TW, Ti-Sa, 30 fs
Intense Laser Irradiation Lab.
Pisa, Italy

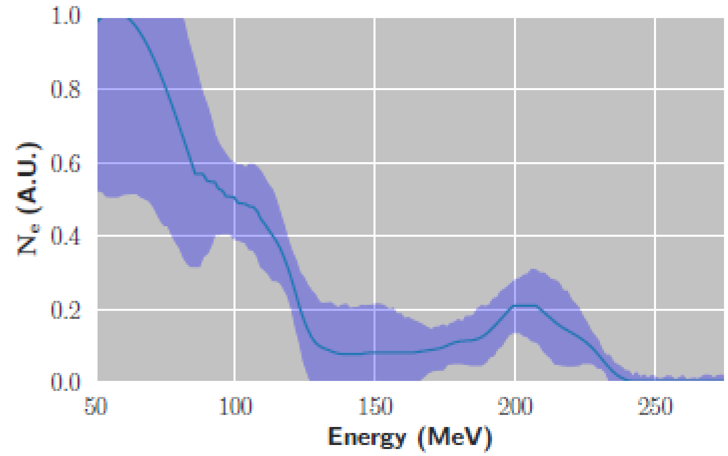

few hundreds of shots → 1-2 Gy

~ 100 pc/shot

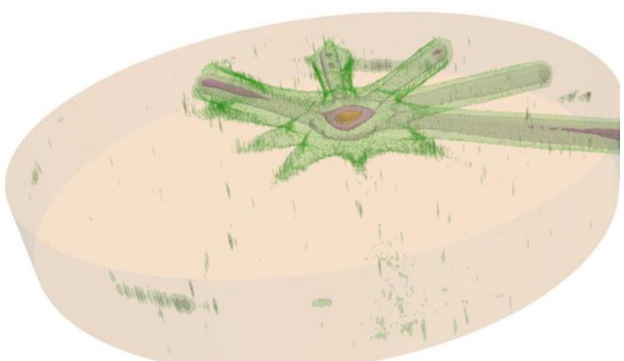

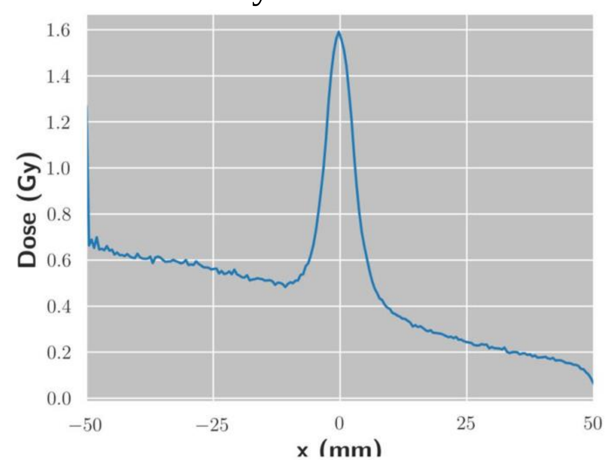

Электронная радиотерапия с использованием лазерного режима релятивистского самозахвата

energy above ~ 50–100 MeV and maximum energy up to ~ 250 MeV

relatively flat spectrum in the region from ~ 100MeV upward

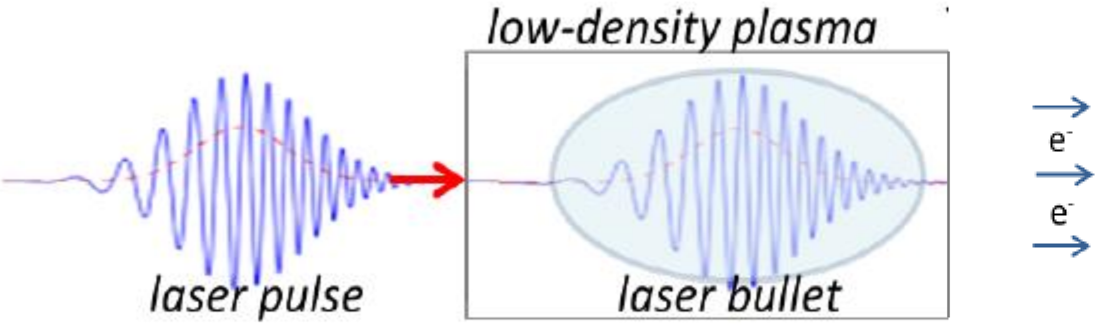

Very universal plateau-type spectra

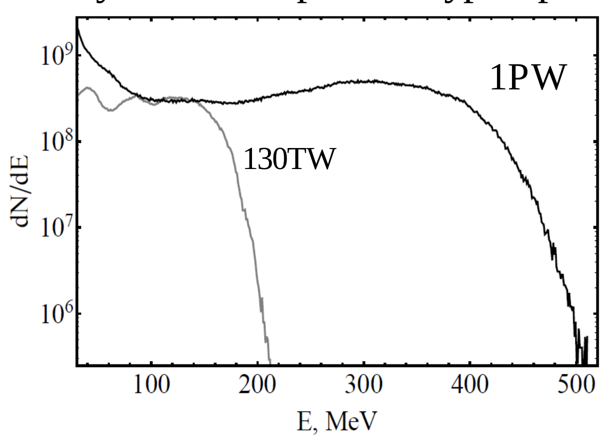

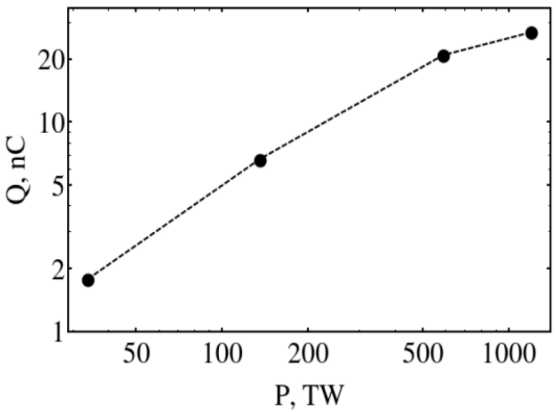

Dependence of the maximum total electron charge on the laser power for a 30 fs pulse

Betatron Motion in LWFA Plasma

Betatron motion in ion channel/cavity/баббл

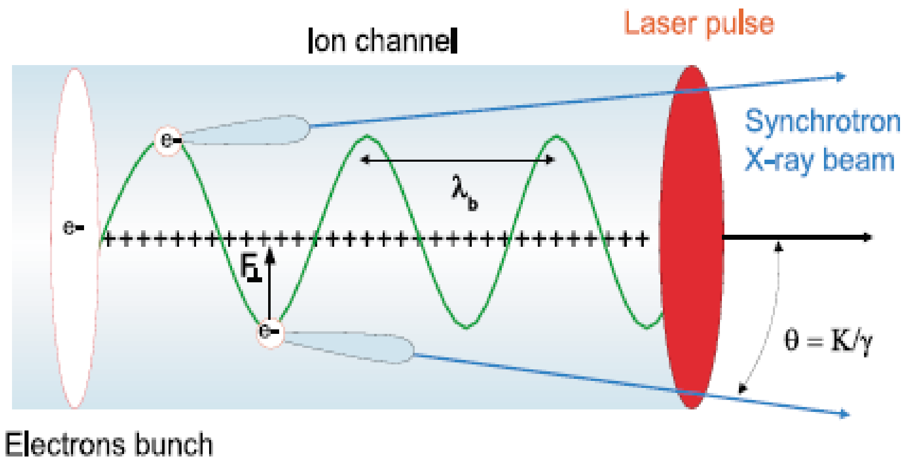

Significant size reduction can be achieved by using LWFA plasma as a source for x-ray beam

Transverse oscillations in the accelerated electron orbits produce betatron radiation

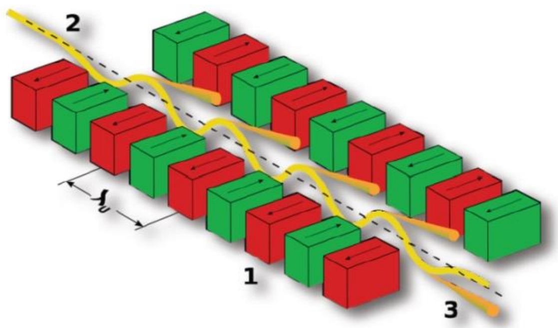

r_β - betatron orbit amplitude (~ 1 μm)

X-ray phase-contrast microtomography

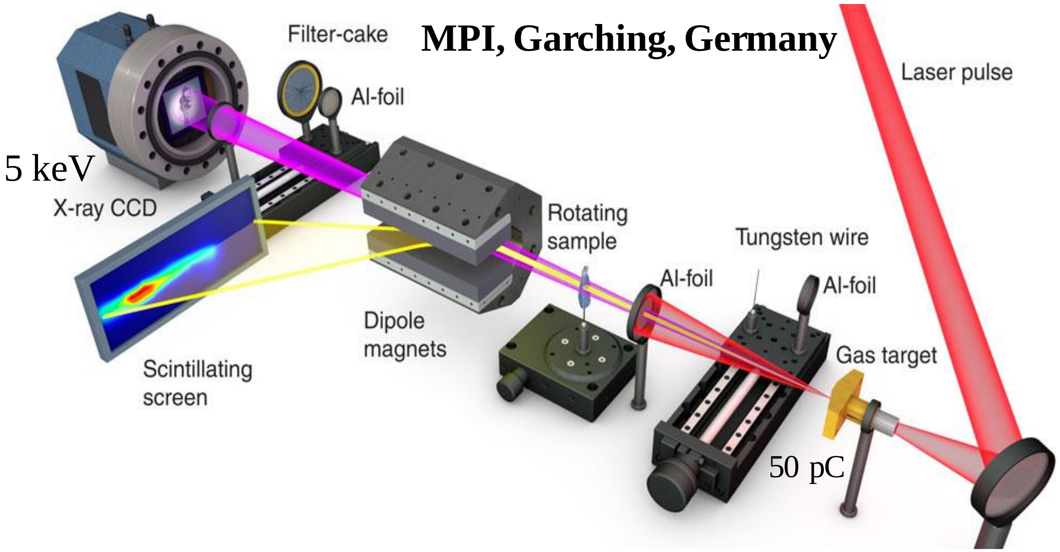

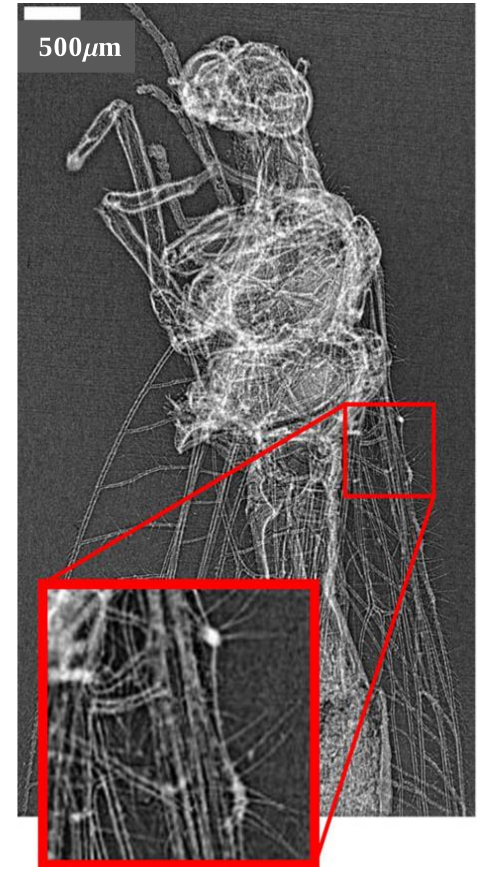

The laser pulse (1.6 J, 28 fs, 60 TW) (red) is focused by a *F*/16 off-axis parabola to a 22-µm diameter spot size on the entrance of a 6-mm long gas cell

Future development -> Detecting cancerous cells among healthy ones (MPI, Garching + Ludwig Maximilian University Munich + Technical University Munich NATURE COMM. (2015) 6:7568).

Biomedical X-ray diagnostics requires scaling multi-TW lasers to kHz reprate:
Reagan, B. A. et al. Demonstration of a 100Hz repetition rate gain-saturated diode-pumped table-top soft x-ray laser. Opt. Lett. 37, 3624–3626 (2012).
Fattahi, H. et al. Third-generation femtosecond technology. Optica 1, 45–63 (2014).

X-ray phase-contrast microtomography

1487 single-shot phase-contrast images, 5-10 keV, N_γ~ (1-2)10^7

Hard x-ray betatron radiation

Источник рентгеновского излучения
повышенной яркости и жесткости

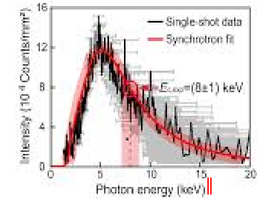

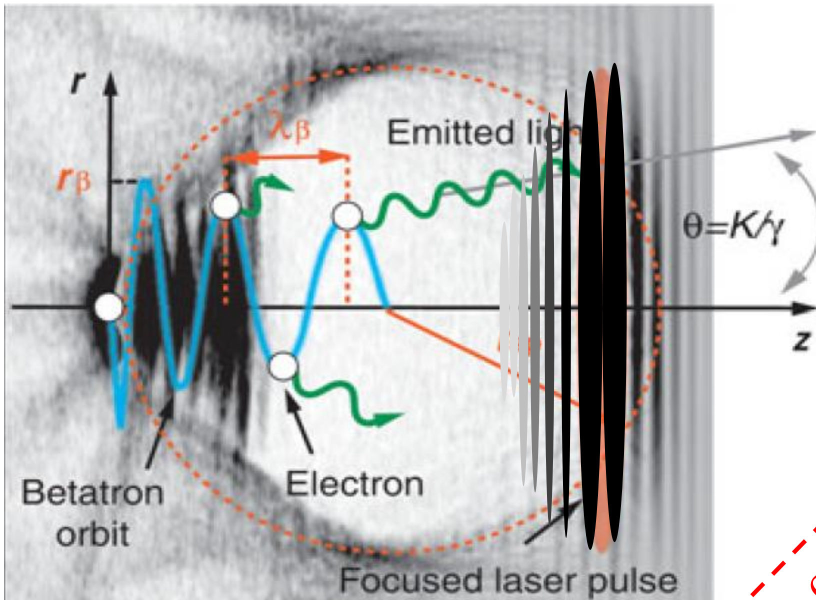

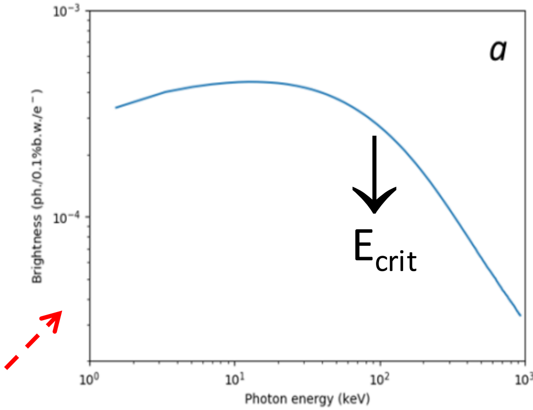

сравни

сравни

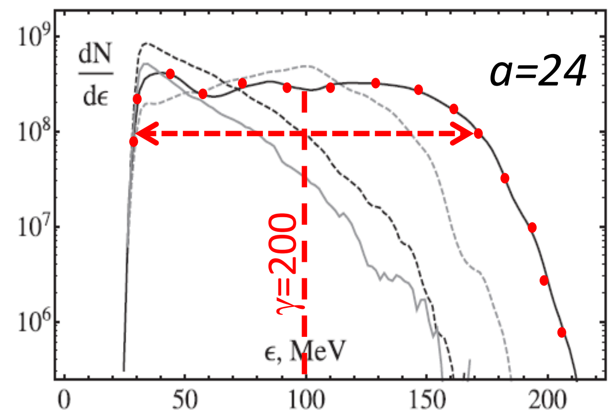

$$E_{crit} = \hbar\omega_{crit} \simeq 5 \times 10^{-24} \gamma^2 (n_e/\mathrm{cm}^{-3})(r_\beta/\mu\mathrm{m})\mathrm{keV}$$

Energy spectra of high-energy (>30 MeV) electrons leaving optimum thickness targets of different densities $1n_c$ (gray curve), $0.75n_c$ (black dashed curve), $0.1n_c$ (black curve), and $0.05n_c$ (gray dashed curve).

$\gamma = 200$, $n_e = 20^{20}$ cm^{-3}, $r_\beta = 5\ \mu$m

$E_{crit} = 100$ keV

Betatron emission I

Randomly chosen (1-1.5)×10^4 trajectories of high-energy electrons
+ Lienard-Wiechert vector potential approach

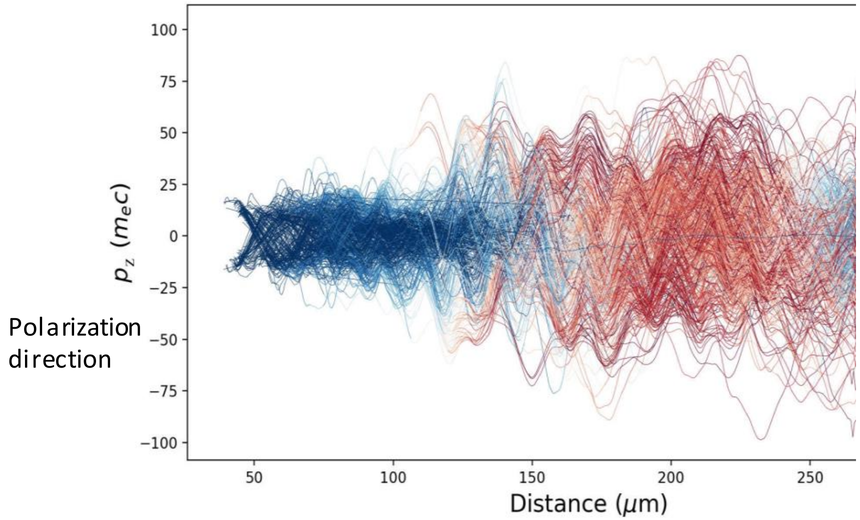

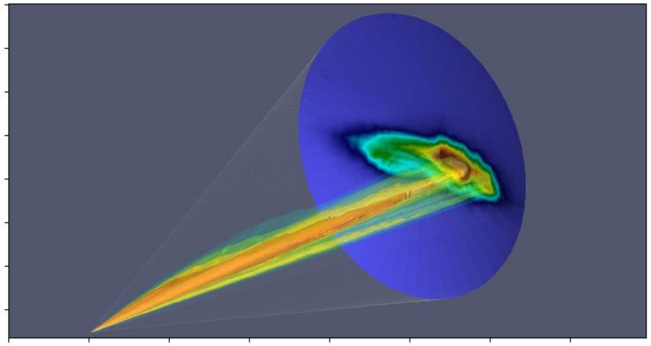

$$a_0 = 24 \rightarrow \simeq 8\times10^{20}\ \mathrm{W/cm^2}$$

130 TW

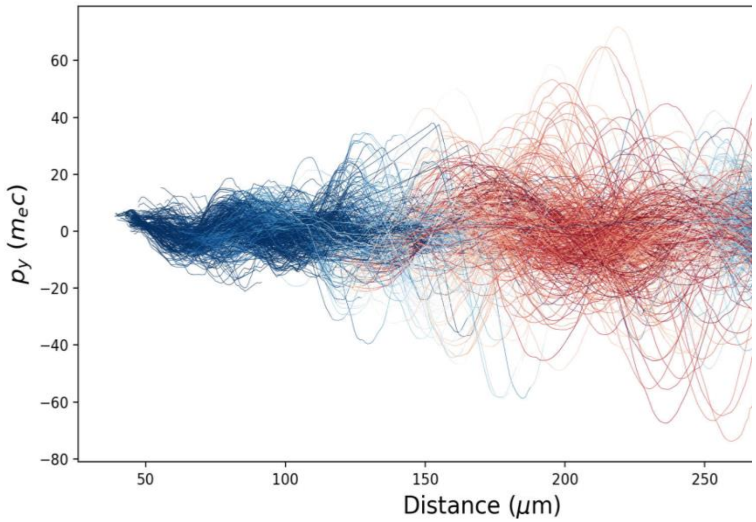

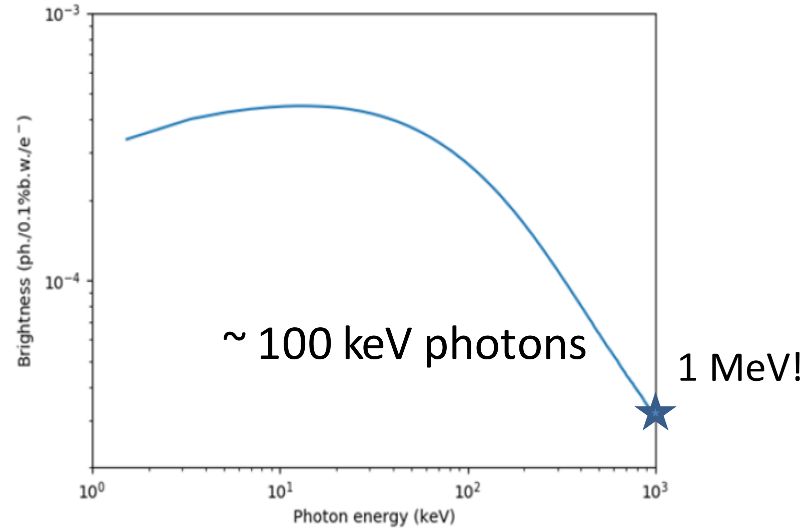

Betatron emission II

peak brightness, > 100keV
10^21 ph/0.1%b.w./mrad^2/mm^2/s

X-ray distribution

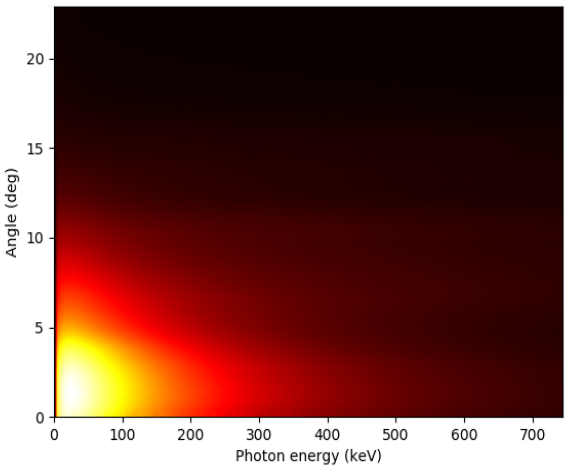

polarization degree, $P \simeq 1/3$.

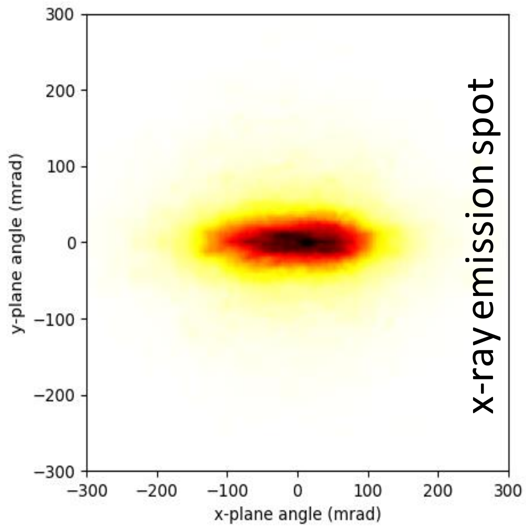

x-ray emission spot

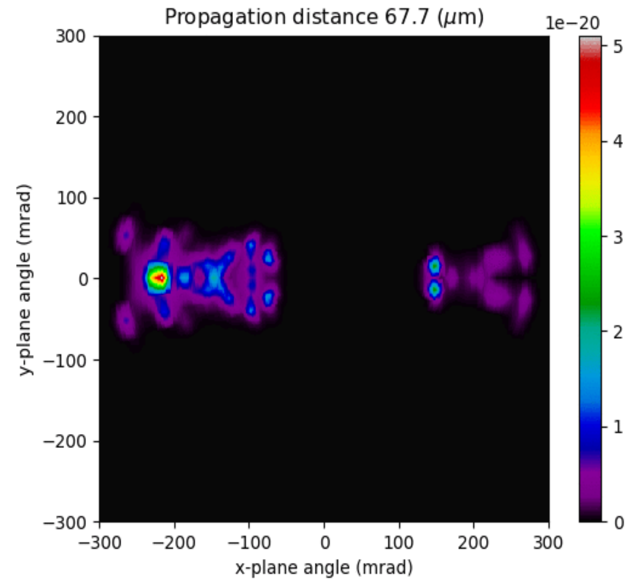

Spectral-angular distribution of the photons (from the electrons with energy > 30 MeV) in a far-field zone.

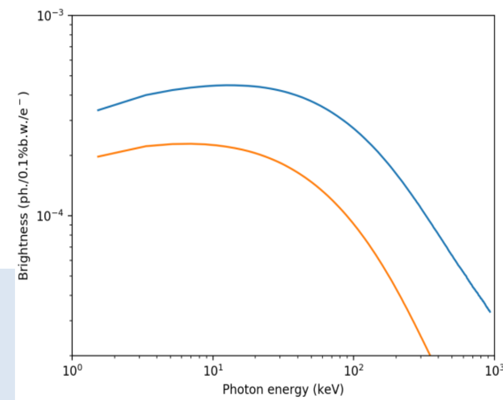

To study magnetic materials
To study local electronic structure

Strongly polarized x-rays

5×10^{10} photons > 10 keV
Photon energy ~ 0.5 m J

Ультрабыстрый имиджинг ударных волн

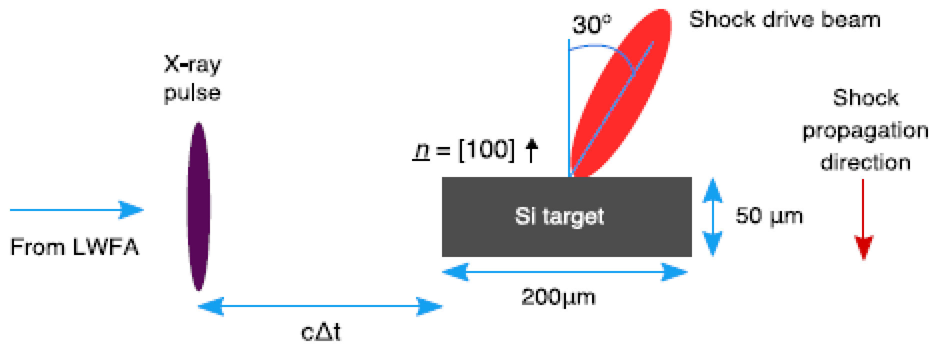

J. C. Wood, et al. Sci.Rep. 8,11010 (2018)

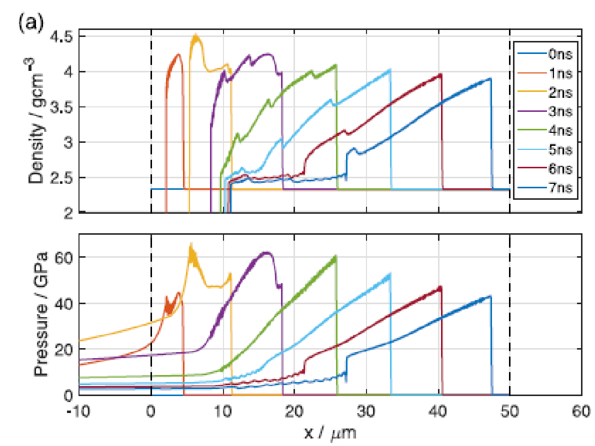

Материалы в экстремальных состояниях (P, T)
валидация расчетно-теоретических моделей

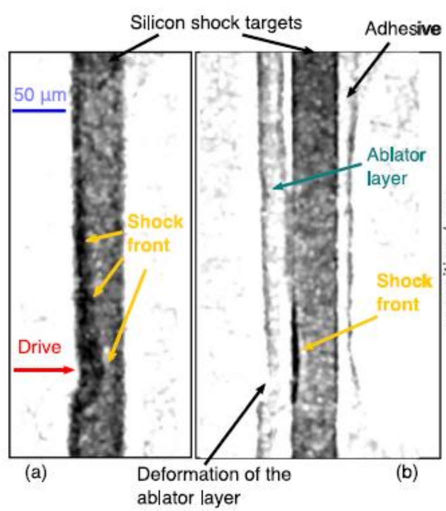

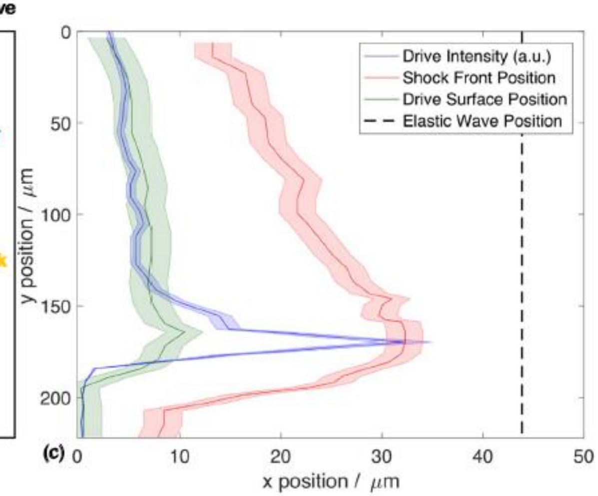

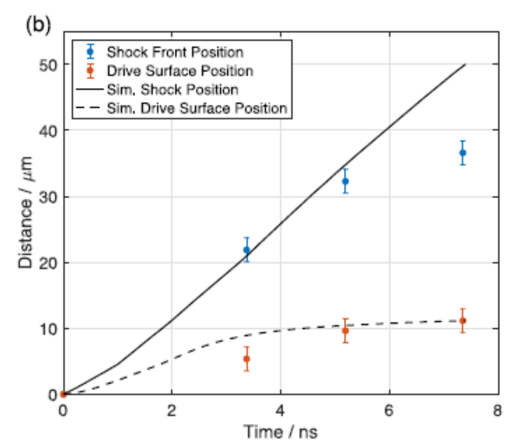

travelling at 8.43 kms^{-1}

A Brilliant Future for Agriculture and Global Food Security

Institut National de la Recherche Scientifique (INRS), Canada

S. FOURMAUX, et al., Optics Express **28**, 3147 (2020)

Throughput X-ray phase contrast plant imaging and screening using LWFA-based X-ray sources

Прямо с грунтом !

Laser →7 J, 18 fs, 2.5Hz

→ X-ray power (40 keV, 30μJ) 10-50 μW → request : ~ 1mJ

Визуальное фенотипирование в селекции растений (оценка роста, заболеваемость (грибок), полиморфизм)

Цифровая селекция!

Optimization of laser-based synchrotron X-ray for plant imaging S. Fourmaux, E. Hallin, P. G. Arnison, J. C. Kieffer, Applied Physics B 125, 34 (2019)

Глубокая экранированная гамма-радиография

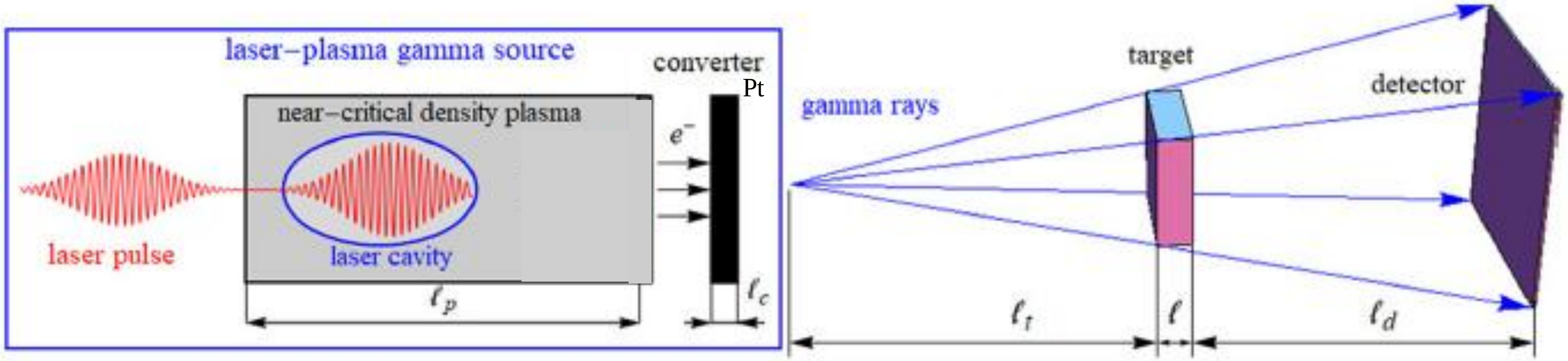

FIG. 1. Schematic diagram of laser-based radiography.

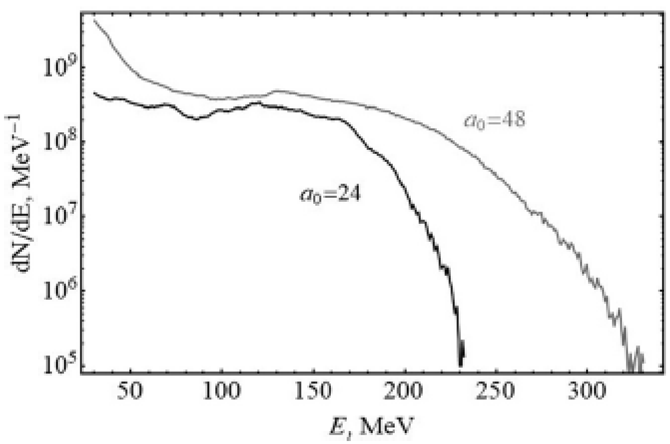

Spectra of accelerated electrons with energy above 30 MeV from the $0.15n_c$ density plasma for a 540 TW laser pulse ($a_0 = 48$) and from the $0.1n_c$ density plasma for a 135 TW laser pulse ($a_0 = 24$) shown by the respective gray and black curves.

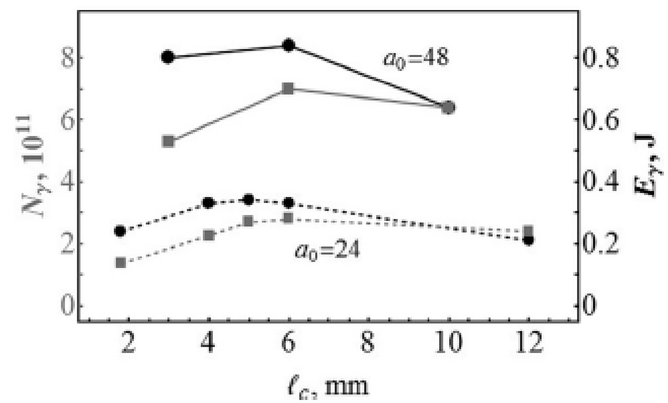

The energy (black curves, right axis) and yield (gray curves, left axis) of gamma rays with the energy above 1 MeV radiated in the forward direction vs the thickness l_c of the Pt converter target for the laser–plasma parameters $P = 540$ TW ($a_0 = 48$) and $n_e = 0.15n_c$ (solid curves) and $P = 135$ TW ($a_0 = 24$) and $n_e = 0.1n_c$ (dashed curves).

For the 135 TW laser, the maximum total yield of gamma radiation is 2.8×10^{11} photons corresponding to a total energy 0.33 J. This is a laser-to-gamma conversion efficiency 8%. The gamma source size ≈ 60 μm for l_c=6 mm and can be reduced to 20 μm by using 2 mm converter. This enables a radiography with tens of micrometers resolution for a sample placed near the gamma source. The electron beam size is the limiting factor for the spatial resolution, typically of 1–2mm

Bremsstrahlung gamma-ray characteristics

Brightness ~10^{19} $s^{-1}mrad^{-2}mm^{-2}$ $(0.1\%BW)^{-1}$

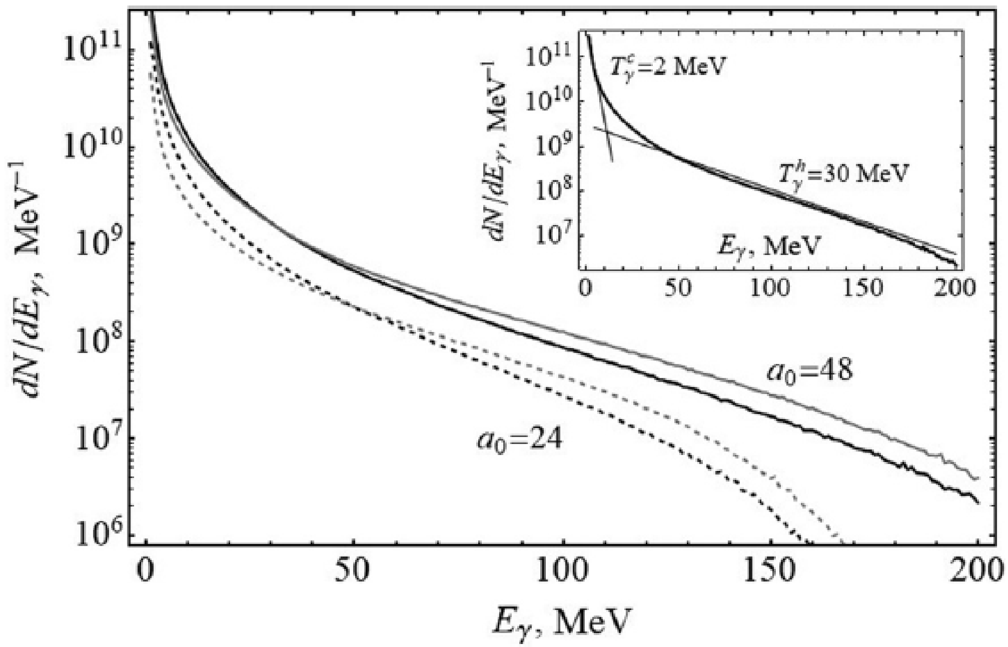

The energy spectra of gamma rays generated in the forward directions from the Pt target of thickness 6 mm (black lines) and 2 mm (gray lines) for the laser–plasma parameters $P = 540$ TW ($a_0 = 48$) and $n_e = 0.15n_c$ (solid lines) and $P = 135$ TW ($a_0 = 24$) and $n_e = 0.1n_c$ (dashed lines). The inset illustrates approximation of the spectrum ($a_0 = 48$, $l_c = 6$ mm) by two-temperature distribution for "cold" and "hot" gammas with the temperatures of $T_\gamma^c = 2$ MeV for the (1–10) MeV photons and $T_\gamma^h = 30$ MeV for the photons with the energies above 40 MeV.

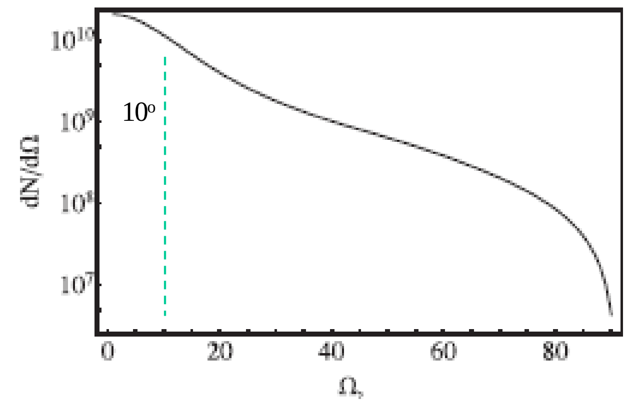

The typical gamma-ray divergence is 150 mrad (10°) with a slightly better collimation for the 540 TW laser.

The photon number in the energy range of (1–2) MeV (10^{10} ph/J) is comparable on the order of magnitude to that in the 3–10MeV energy range.

GAMMA RADIOGRAPHY OF SAMPLES LOCATED DEEP IN A DENSE MEDIUM

M.G.Lobok, A.V.Brantov, and V.Yu.Bychenkov
Phys. Plasmas **27**, 123103 (2020)

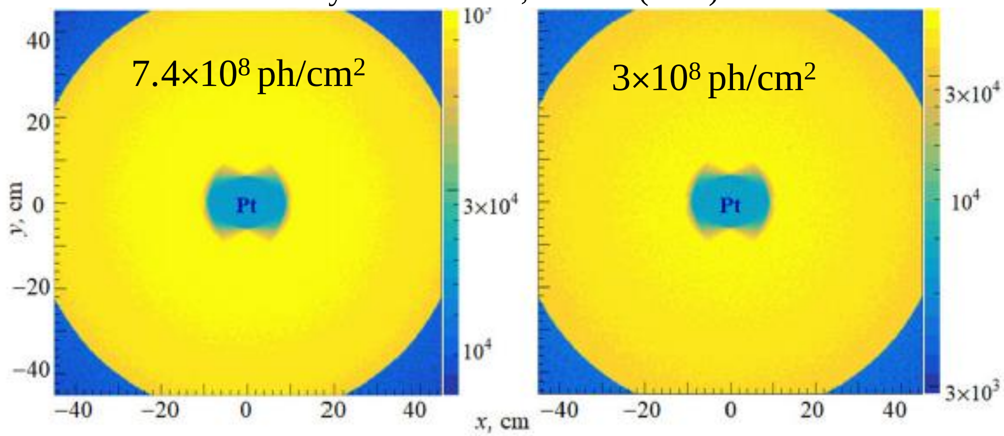

FIG. 6. Simulated radiography images (cm × cm) of the shielded crumpled platinum tube surrounded by a 3 cm thick iron shell (case 1) from the gamma source based on the 540 TW laser (left) and 130 TW laser (right). The legend presents number of photons per one detector pixel (with the size of 3 mm × 3 mm).

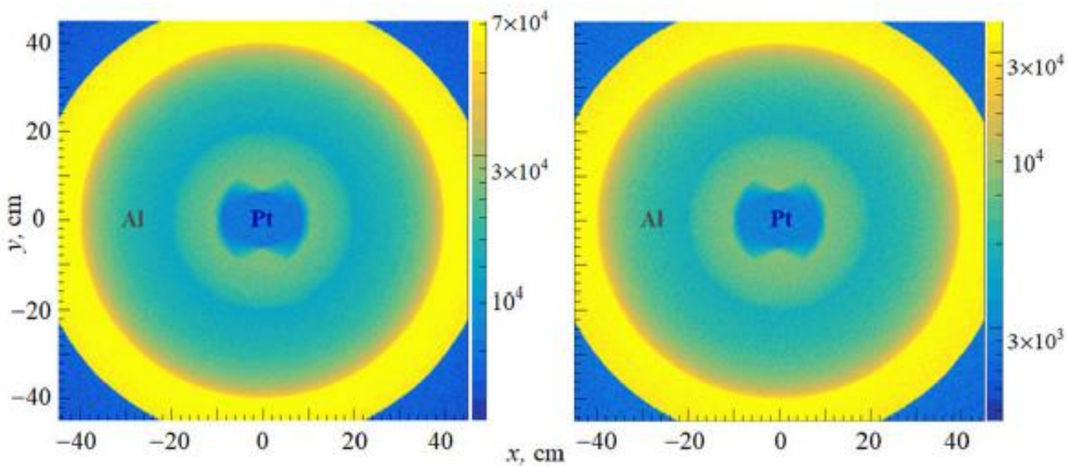

The same as in Fig. 6 but for case 2.

$l_t = l_d = 5m$,
gamma image contrast $C = 0.9$

Case 1: iron shell of thickness 3 cm with an inner radius 47 cm surrounding the sample.
Case 2: additional 10 cm Al with an inner radius 10 cm.

Discrimination between high-Z and medium-Z material several γ MeV is needed, i.e. isotope radioactive γ-sources (60Co at 1.17MeV and 1.33MeV) for cargo screening do not fit this. Their penetration ability is also limited due to not high enough gamma energy.

Compton (Thomson) Scattering as a Gamma Source

$$\lambda' = \lambda(4\gamma^2)^{-1}$$

electron ~ 250 MeV | photon ~1 eV | scattered photon ~1 MeV

- Mechanism well-studied since 1960s
- Cross-section 600mb
- Radiation opening angle ~1/γ
- Considered for short gamma ray source

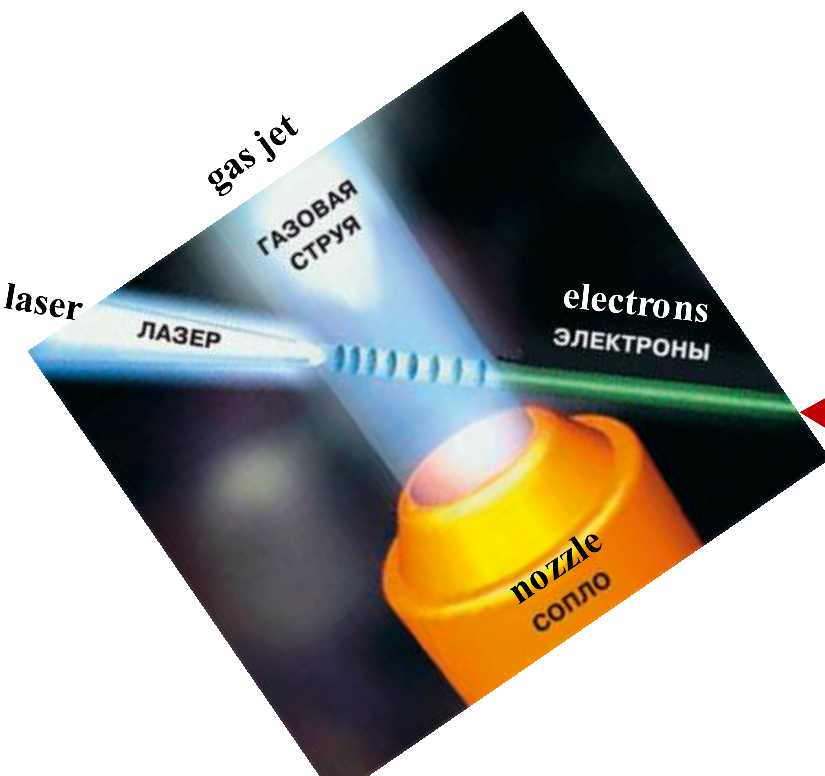

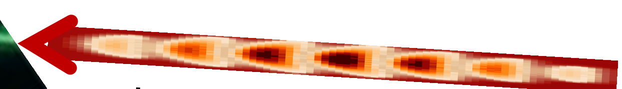

Laser beam to be scattered

T-REX MEGa-ray source:

nuclear materials detection system;
– needed to study isotopes;
T-REX is the world's highest peak brightness up to 2 MeV light source.

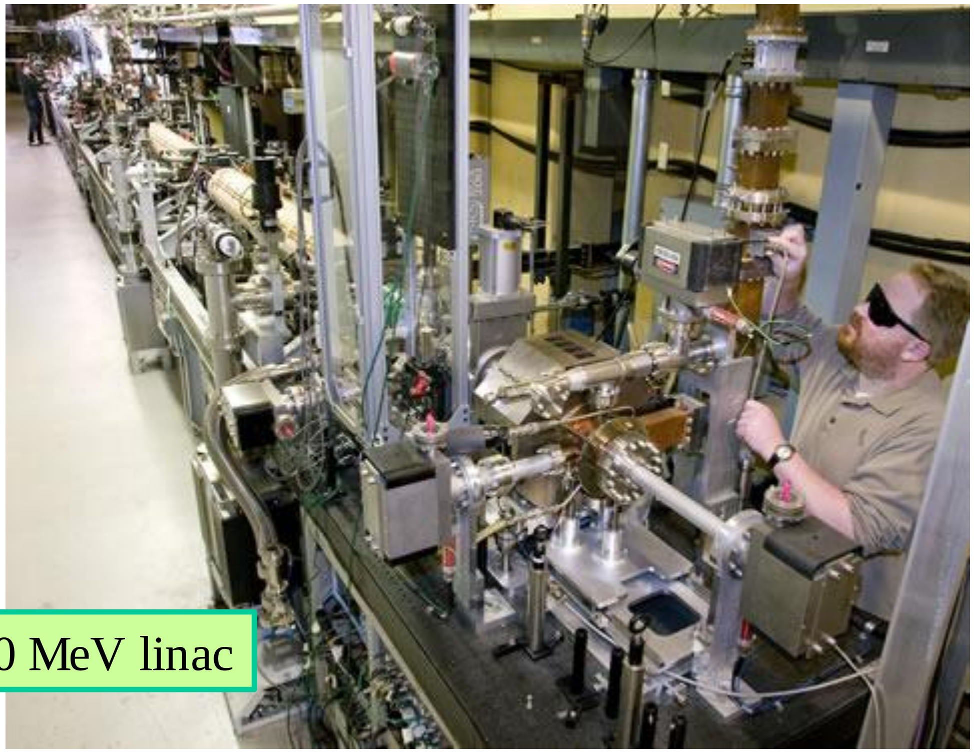

120 MeV linac

The diode pumped ILS will deliver 0.5 J, 10 ps pulses at 120 Hz repetition rate, at 1064 nm (532 nm)

F. Albert et al., OPTICS LETTERS **35**, 354 (2010)
Detection of LiH shielded by Pb and Al is accomplished using nuclear resonance fluorescence line of 7Li at 478 keV.

Development of MEGa-ray Technology at LLNL

ELI NP

Dr. C. P. J. Barty
Chief Technology Officer
National Ignition Facility & Photon Science Directorate
Lawrence Livermore National Laboratory
Livermore, California

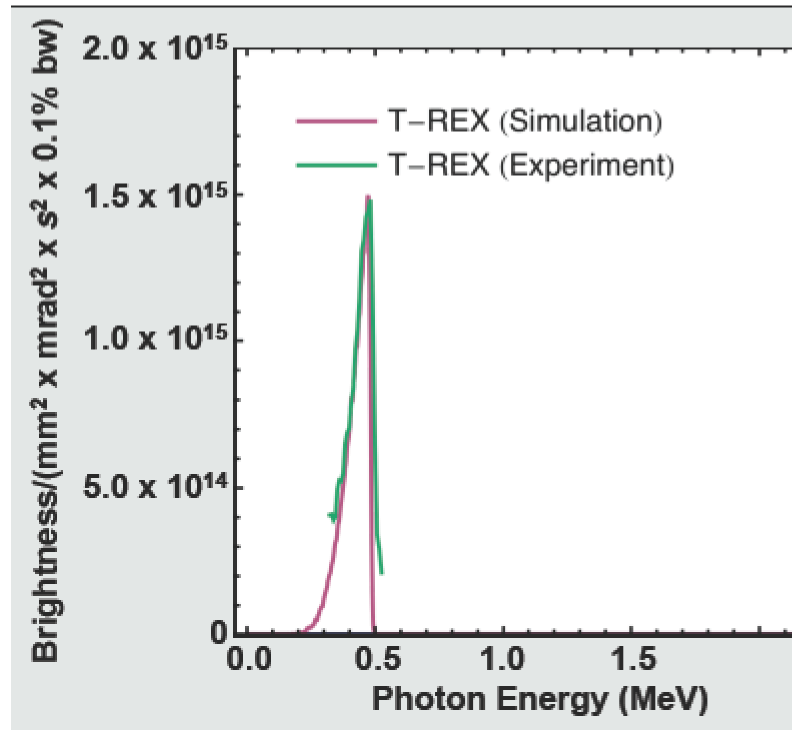

Measured and expected spectra

Полностью оптический комптоновский источник

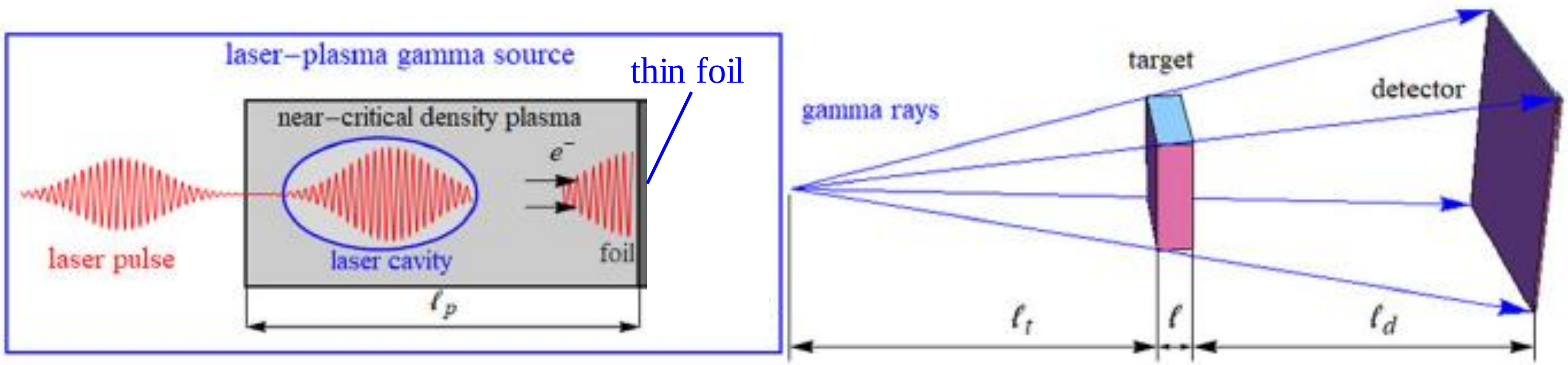

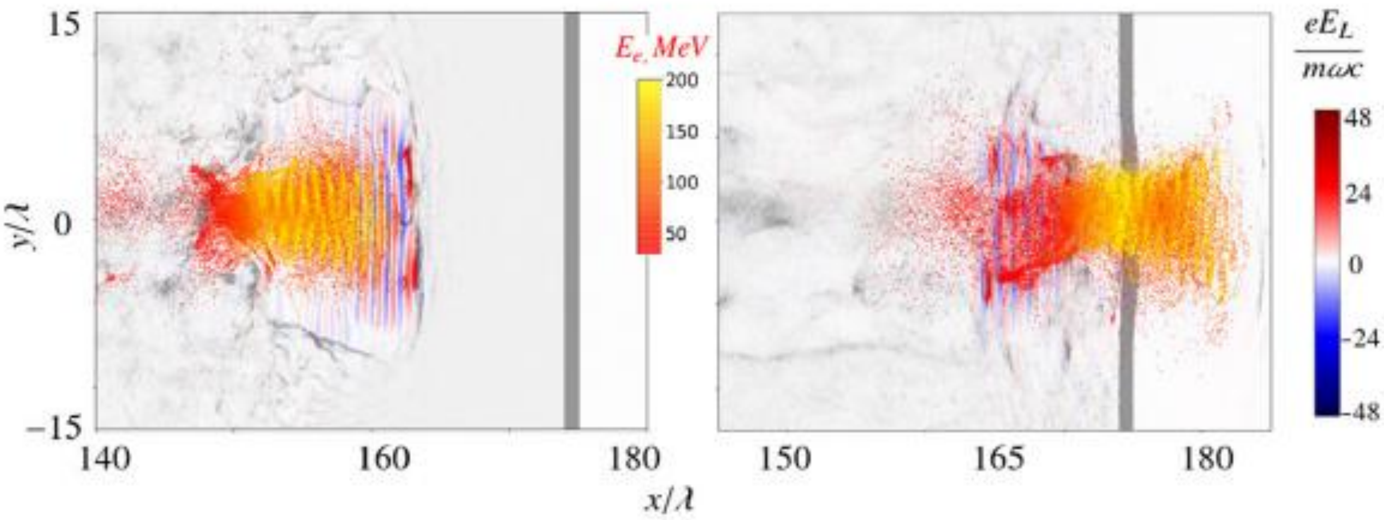

Electromagnetic field and electron density (in gray) at the instant 635 fs before reflection of the laser pulse (left) and at the instant 710 fs after reflection, when the electron bunch has already penetrated through the reflected pulse and has appeared behind the target (right). Electrons with energies >30 MeV are highlighted.

Characteristics of the all-optical Compton source

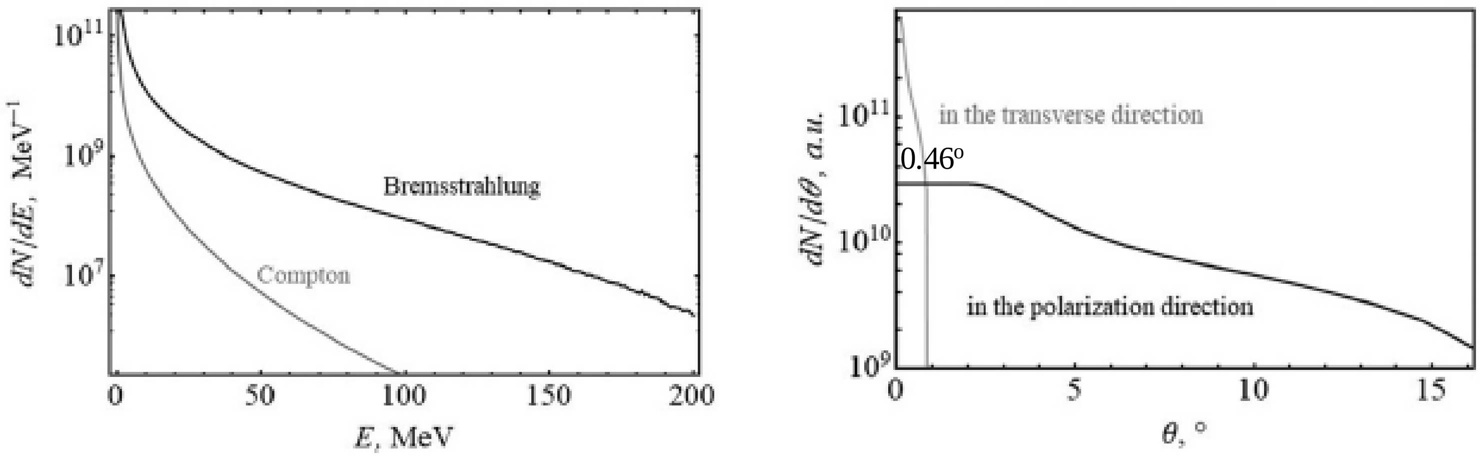

The energy spectra (left panel) of gamma rays generated by nonlinear inverse Compton scattering (gray curve) compared with the bremsstrahlung gamma spectrum from the Pt target of thickness 6mm (black curve) and the angular distribution of Compton gamma quanta (right panel) in the laser polarization direction (black curve) and in the transverse direction (gray curve) for the laser–plasma parameters $P = 540$ TW ($a_0 = 48$) and $n_e = 0.15n_c$.

Rather a small flux of photons from the inverse Compton source do not fit well a single-shot heavy shielded radiography of large objects, but demonstrates ability of single-shot radiography of small-size dense samples

High gamma-ray brightness ~7×10^{20} $s^{-1}mrad^{-2}mm^{-2}$ $(0.1\%BW)^{-1}$ (almost two order of magnitude higher than for bremsstrahlung source)

Комптоновская гамма-радиография

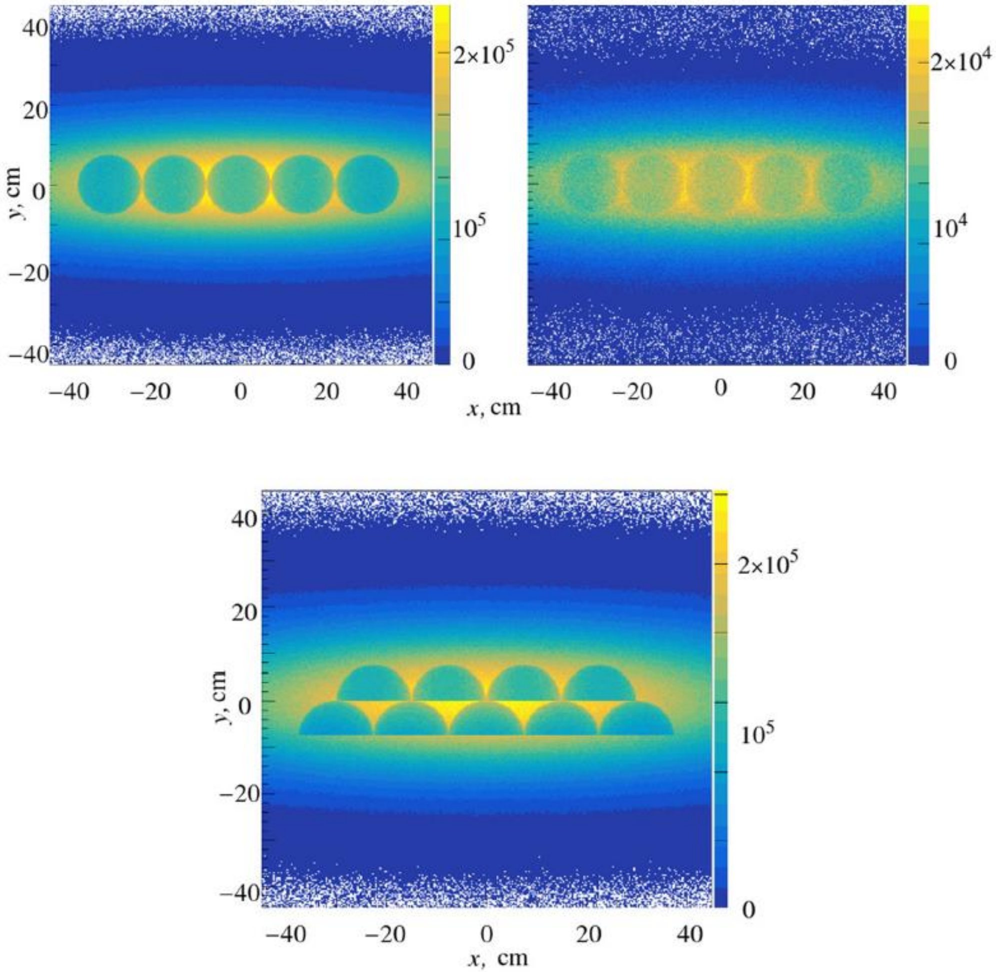

l_t=20 cm,
l_d=10 m,
r_{Pt} = 1.5 mm

Simulated radiography images (cm × cm) of the platinum mm ball chain (upper left) and the same inside a 3 cm-thick iron shell (upper right) and two platinum chains (bottom) from the inverse Compton gamma source based on the 540 TW laser. The legend presents the number of photons per one detector pixel (of the size 3

Gamma image contrast is C = 0.6 for the unshielded sample and the shielding by the iron shell reduces the image contrast to C = 0.3-0.4.

Positron Creation Using Ultra-intense Lasers

Tokamaks	Penning-Malmberg Traps	Ultra-intense Lasers
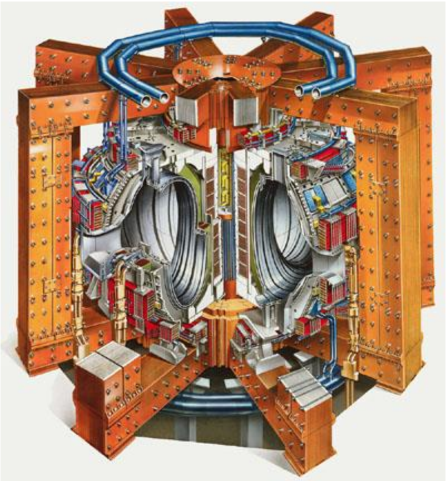	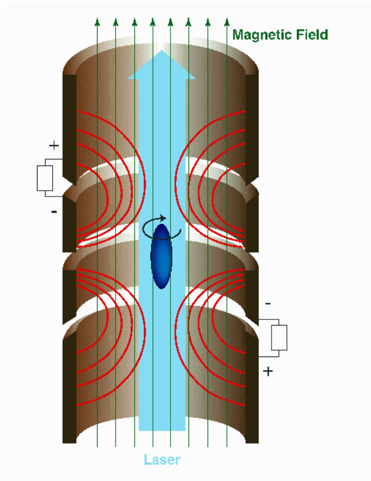	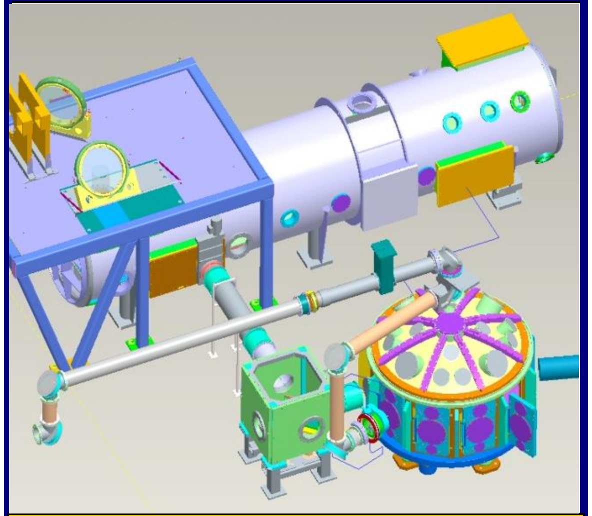
Theory only $N_{e+} \sim 8\text{x}10^{14}$ $V \sim 2.7 \text{ x } 10^7 \text{ cm}^3$	Experimental $N_{e+} \sim 8\text{x}10^7$ V ~ 6 cm x 1 mm(D.)	Titan laser $N_{e+} \sim 10^{11}$ V ~ 1 mm x 1 mm(D.)
$3.3 \text{ x } 10^7 \text{ cm}^{-3}$	$4 \text{ x } 10^9 \text{ cm}^{-3}$	$1 \text{ x } 10^{14} \text{ cm}^{-3}$

Could lasers create the highest density of positrons in the laboratory, by creating a large number in a short time (~ picosecond) ?

Two main processes involved in laser positron creation in the presence of high-Z nucleus

1. Direct (Trident) pair production
   $e^- + Z \rightarrow 2e^- + e^+ + Z$
   (*Z:* nucleus)
2. Indirect (Bethe-Heitler) pair production:
   $e^- + Z \rightarrow \gamma + e^- + Z$
   $\gamma + Z \rightarrow e^- + e^+ + Z$
   (γ: Bremsstrahlung)

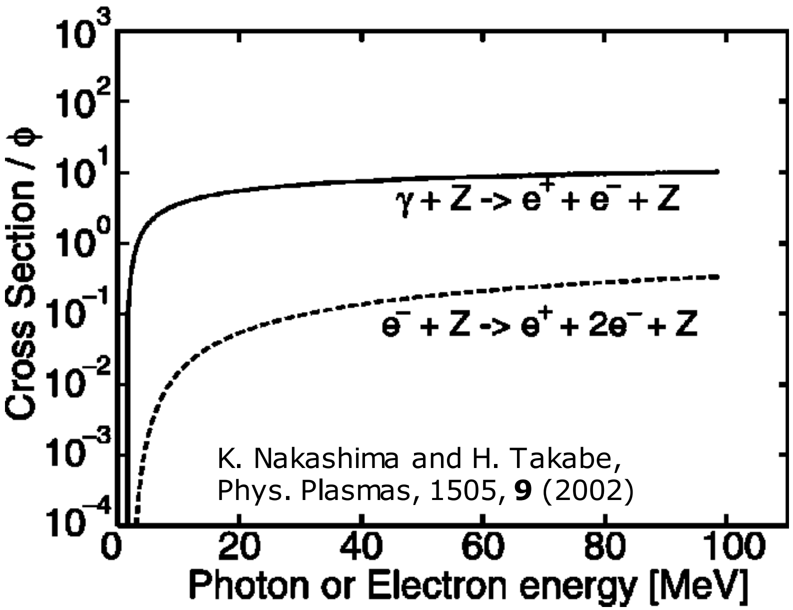

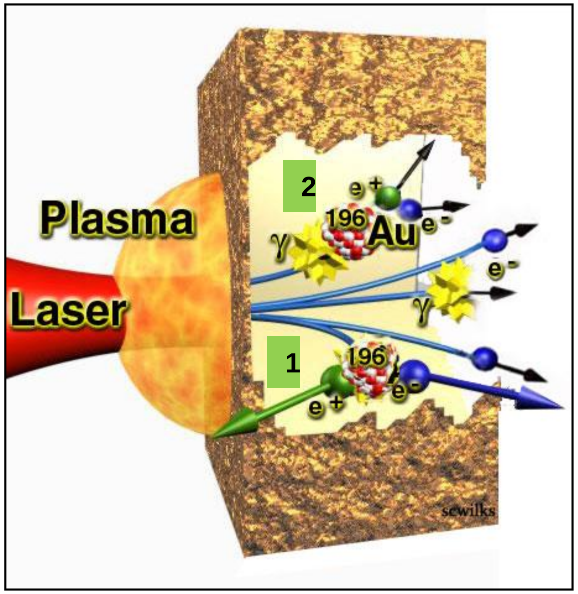

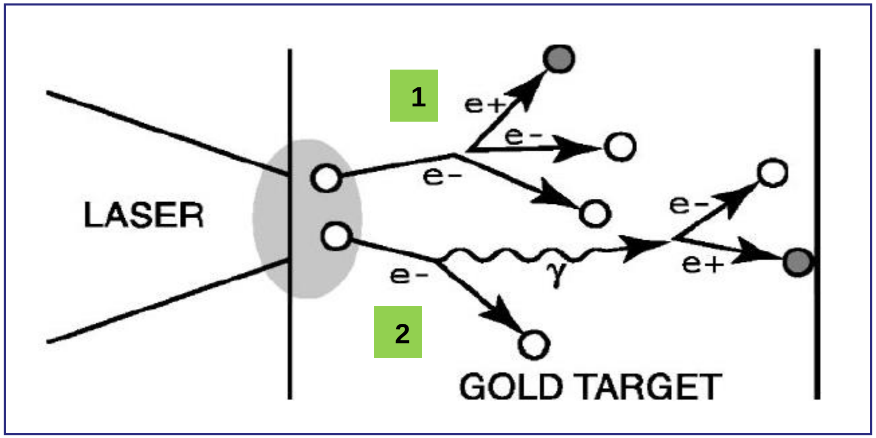

High energy (>MeV, relativistic) *e*-s are the key to both processes

Positron generation

Bether-Heitler

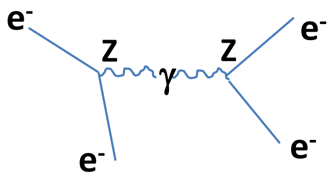

>

Trident

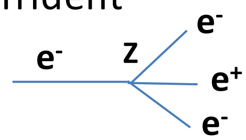

$n_{e+}=2\times10^{12}\ cm^{-3} \rightarrow n_{e+}/4J = n_{e+}/150J$ ("Titan")

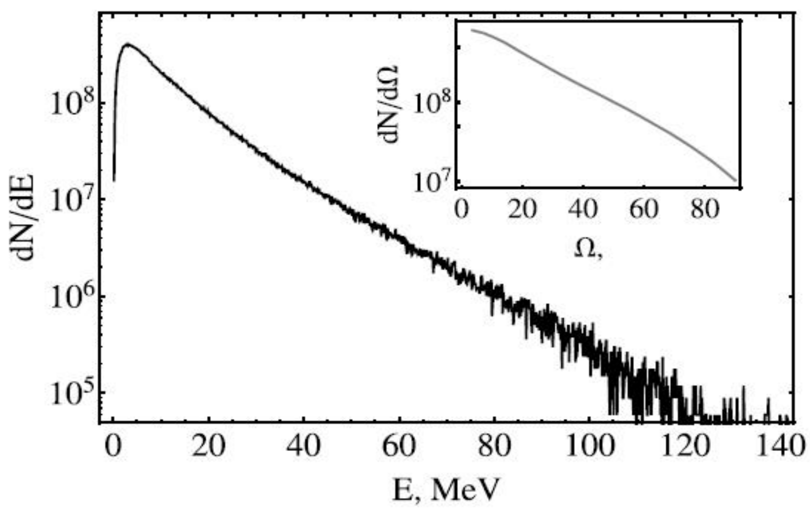

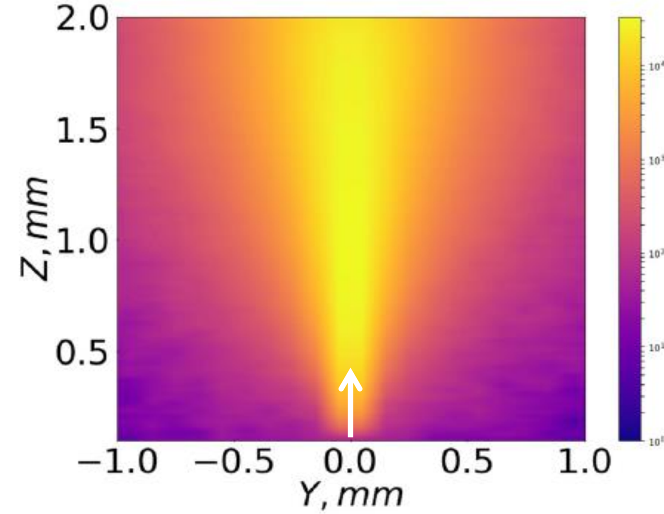

Energy spectrum of positrons generated from a 6 mm Pt target (left panel) and positron flux in a 1.8 mm Pt target (right panel) for the laser–plasma parameters $P = 130$ TW, $R_L = 2\lambda$, and $n_e = 0.1 n_c$ corresponding to an electron bunch with $Q \simeq 7$ nC and an average energy of 100 MeV. The inset in the left panel shows the angular distribution of positrons generated from the 6 mm Pt target.

$N_{e+} = 9\times10^9$ 6 mm thick Pt target $N_e >> N_{e+}$

The positron jet angular spread increases from ~20° for a 1.8mm Pt converter target to ~35° for a 6mm target and ~40° for a 12mm target.

Electron conversion to neutron emission

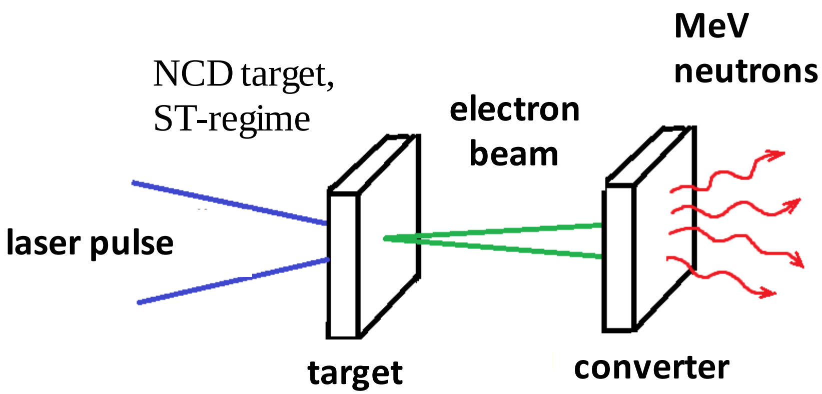

$8\times10^{20} W/cm^2, \lambda=1\mu m,$ *30fs,*
$d=4\mu m,\ n_e=0.1n_c,\ Q=7nC$

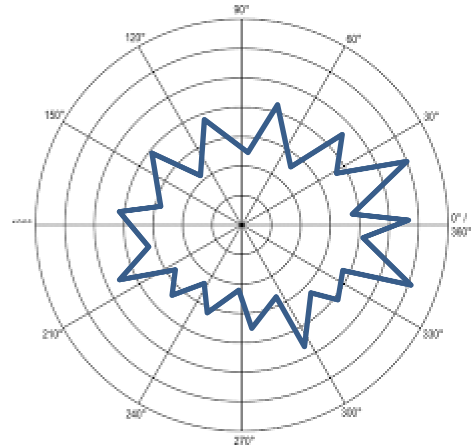

nearly isotropic
neutron
distribution

2×10^8 n°
↓
5×10^7 n°/J

6×10^{-3} neutrons/electron

giant dipole resonance (GDR), 10 – 20 MeV

dominance

(γ,n), (γ,2n), (γ,np), (γ,3n), …..

highrep laser is
required (kHz)

$K_n \sim 5\times10^{-4}$

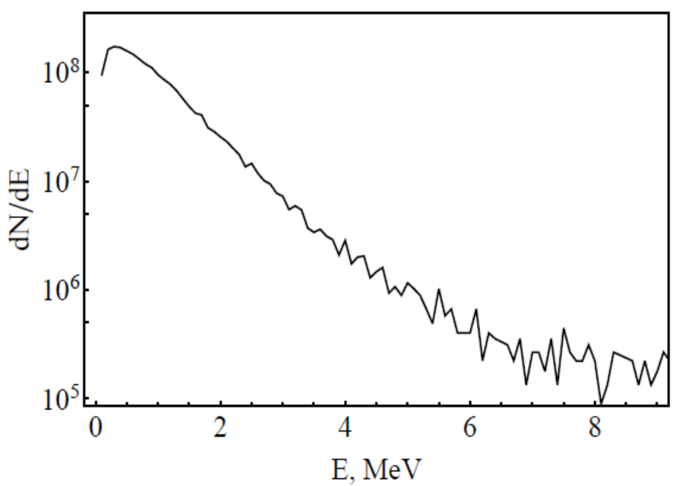

Energy spectrum of neutrons generated from a 12 mm thick Pt target outside the target the forward and backward directions (at a 108° angle in both cases)

In general, photonuclear cross-section is smaller than typical nuclear cross sections due to the electromagnetic nature of interaction. However, at the resonance energy it is comparable on the order of magnitude with the geometrical nuclear cross section that well compensate a weakness of electromagnetic interaction.

PET isotope production (^{64}Cu)

^{65}Cu (γ,n)^{64}Cu →64Ni + e+ регистрация 2-х одинаковых разлетающихся фотонов (позитронно-эмиссионная томография ≡ двухфотонная эмиссионная томография)

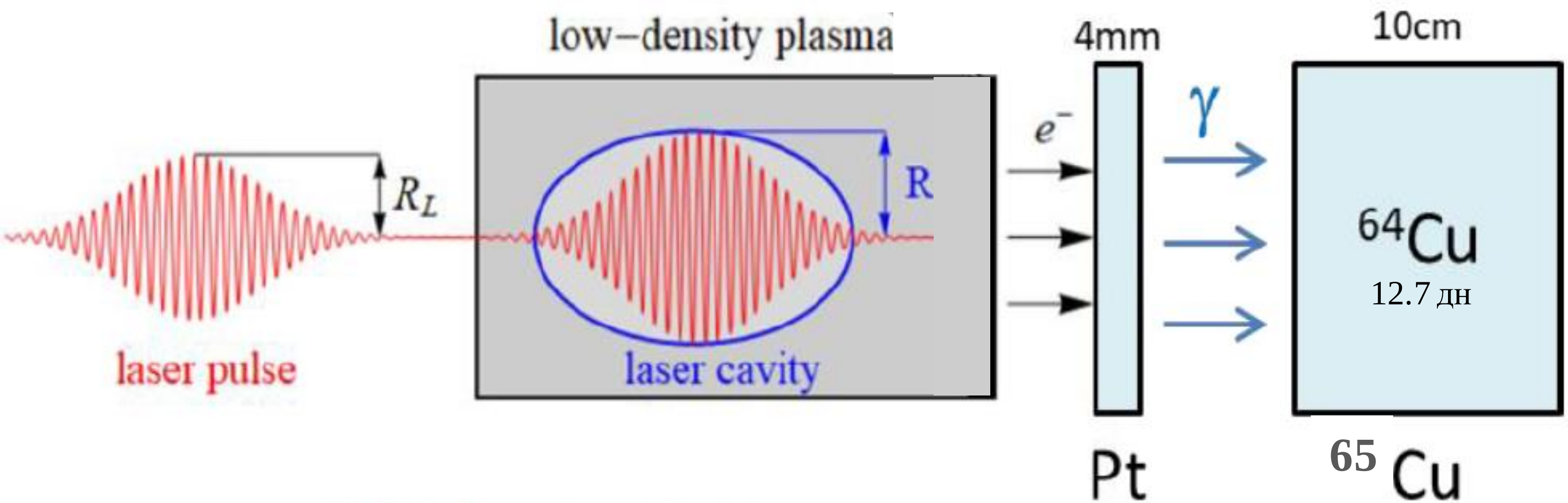

parameters: P=130 TW, focal spot size = 6μm, pulse duration = 30 fs, plasma electron density = $0.1n_c$. **The yield of the isotope ^{64}Cu is 3×10^8**, that is unattainable for the reaction ^{64}Ni + p from a perfectly optimized scheme with an ultrathin solid dense foil (A.V.Brantov et al., Phys. Rev. AB 18, 021301 (2015)).

SPECT isotope production (^{111}In) – однофотонная эмиссионная томография

$$^{112}Sn\,(\gamma,n)\,^{111}In, \qquad ^{111}In + e^- \xrightarrow{2.83\ \text{дн.} \to \gamma} {}^{111}In^* + \nu_e, \quad {}^{111}In^* \to \gamma$$

Захват электронов

Photoproduction of mesons

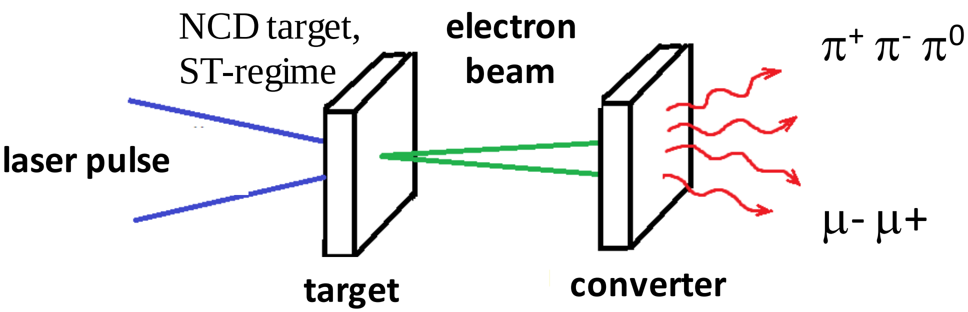

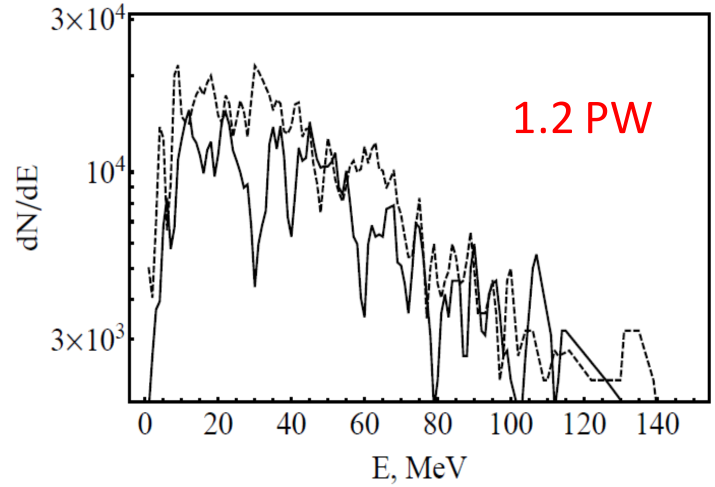

Spectra of photonuclear generated π^+ (solid line) and π^- (dashed line) pions

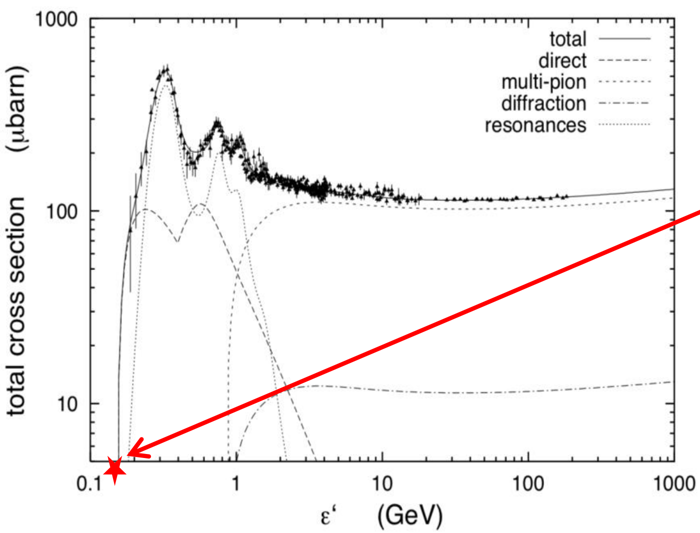

130 TW

$\pi^+ \approx \pi^0$ => 160, π^- => 210

Σ = 530

Cf. W. Schumaker et al., *New J. Phys.* **20**, 073008, 2018

1.2 PW

$\pi^+ \approx \pi^0$ => 7×10^5, π^- => 1×10^6

unstable

$\Sigma = 2.4\times10^6$

μ^- μ^+ pairs
were detected
only from several PW pulse

Трансмутация долгоживущих изотопов

Greenpeace estimates there are roughly 250,000 tons of nuclear waste in 14 countries across the world. Of that, about 22,000 cube meters is hazardous. The cost of storing it all, according to GE-Hitachi, is more than $100 billion, (discounting China, Russia, and India).

1 Ma = 1 млн. лет	
^{129}I	15.7 Ma
^{107}Pd	6.5 Ma
^{135}Cs	2.3 Ma
^{93}Zr	1.53 Ma
^{79}Se	0.327 Ma
^{126}Sn	0.230 Ma
^{99}Tc	0.211 Ma

photo-transmutation of 129I with a half-life of 15.7 million years to 128I with a half-life of 25 min

$$^{129}\mathrm{I}(\gamma,n)^{128}\mathrm{I}$$

K. W. D. Ledingham et al., Laser-driven photo-transmutation of 129I – a long-lived nuclear waste product, J. Phys. D: Appl. Phys. 36 (2003) 79.

Gérard Mourou

ELI – Beamlines and **ELI**-NP
Extreme Light Infrastructure

By further increasing the pulse power of the laser via the CPA technique, Gérard Mourou sees applications such as the transmutation of radioactive elements contained in some of the most radioactive and long-lived waste.

Структурированные мишени суб-микронного масштабы для получения рентгеновского излучения и нейтронов

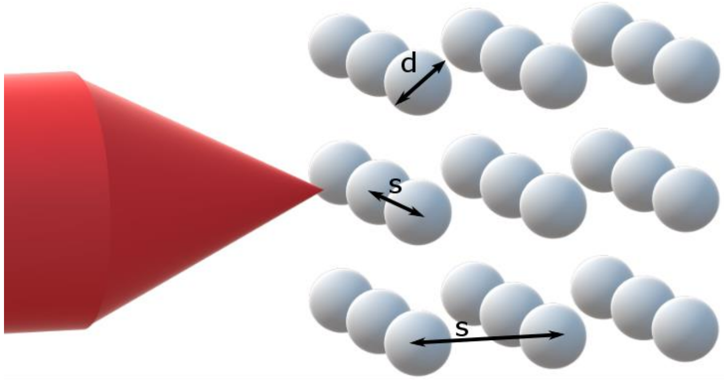

Стохастический нагрев в сложных полях, рассеяние на большие углы, согласование eφ~ Te ($\propto a_0$), блуждающие электроны, кулоновский захват

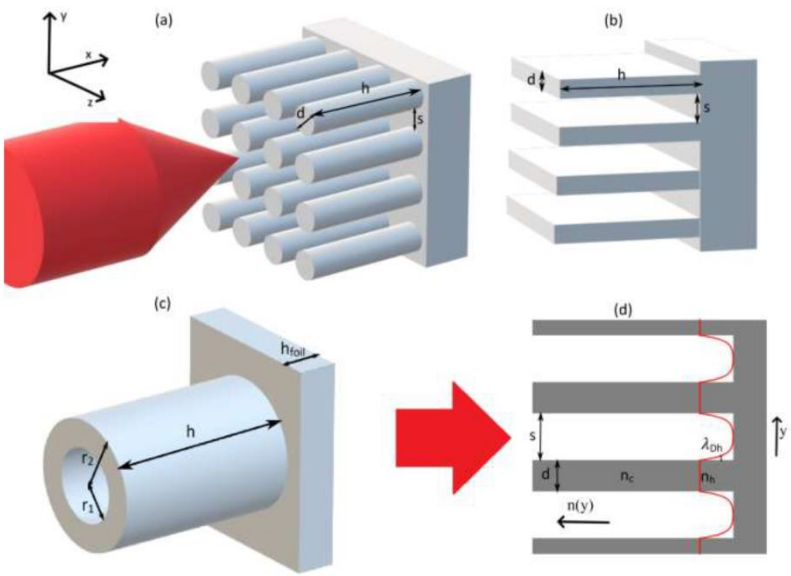

Высокая средняя плотность, прозрачность для света, почти полное поглощение

Выводы

Радиационные и ядерные применения

Первопринципные эксперименты → оптимизационные эксперименты

Электронная радиотерапия (радиография)

Источник жесткого рентгеновского излучения

Экранированная гамма-радиография

Полностью оптический комптоновский источник

Фотоядерные реакции. Получение нейтронов

Лазерный источник элементарных частиц

Получение медицинских изотопов

Трансмутация долгоживущих изотопов


Спасибо
За внимание!